

Fred Dolan EW14

SPACE SHUTTLE MAIN ENGINE  
(SSME) LOX TURBOPUMP PUMP-END  
BEARING ANALYSIS

FINAL REPORT

{NASA-CR-178746} SPACE SHUTTLE MAIN ENGINE N86-22633  
{SSME} LOX TURBOPUMP PUMP-END BEARING  
ANALYSIS Final Report (Spectra Research  
Systems, Inc.) 60 p HC A04/MF A01 CSCI 21H  
G3/20 16840  
Unclas



**SRS**  
TECHNOLOGIES

SRS/STD-TR86-007  
535

SPACE SHUTTLE MAIN ENGINE  
(SSME) LOX TURBOPUMP PUMP-END  
BEARING ANALYSIS

FINAL REPORT

JANUARY 6, 1986

SUBMITTED BY: SRS Technologies  
555 Sparkman Drive, Suite 1406  
Huntsville, AL 35805

PREPARED FOR: Mr. Fred J. Dolan  
Materials and Processes Laboratory  
Engineering Physics Division  
George C. Marshall Space Flight Center  
Marshall Space Flight Center

CONTRACT NUMBER: NAS8-36183 Modification No. 6



SYSTEMS TECHNOLOGY DIVISION

555 SPARKMAN DRIVE/SUITE 1406  
HUNTSVILLE, ALABAMA 35805  
(205) 830-0375

TABLE OF CONTENTS

SECTION	PAGE
FOREWORD. . . . .	ii
TABLE OF CONTENTS . . . . .	iii
LIST OF FIGURES . . . . .	iv
LIST OF TABLES. . . . .	v
1.0 INTRODUCTION. . . . .	1
2.0 SUMMARY . . . . .	2
3.0 SHAFT/BEARING MODEL DESCRIPTION . . . . .	4
3.1 SHABERTH Shaft/Bearing Model . . . . .	4
3.2 SINDA Thermal Model of 45 mm Bearing . . . . .	4
3.3 Model Iteration Process. . . . .	6
4.0 ANALYSIS OBJECTIVES AND APPROACH. . . . .	9
5.0 ANALYSIS RESULTS. . . . .	13
5.1 Mechanical Characteristics . . . . .	13
5.2 Thermal Analysis Results . . . . .	15
6.0 CONCLUSIONS AND RECOMMENDATIONS . . . . .	52

LIST OF FIGURES

FIGURE NUMBER		PAGE
3.1.1	SSME LOX Turbopump Bearing/Shaft Load Configuration. . . . .	5
3.3.1	Iteration Process Between SHABERTH and SINDA . . . . .	7
3.3.2	Example of a Diverged Iteration Process. . . . .	8
4.1	Parameter Data Tree with Nominal Heat Transfer Coefficient . .	10
4.2	Parameter Data Tree with Enhanced Heat Transfer Coefficient. .	11
5.2.1	45 mm Bearing Operating Temp. Vs. Axial Preload. . . . .	20
5.2.2	45 mm Pump End Bearing Operating Temperatures Vs. Axial Preload. . . . .	21
5.2.3	45 mm Bearing Operating Temperatures Vs. Axial Preload . . . .	22
5.2.4	45 mm Bearing Operating Temperatures Vs. Axial Preload . . . .	23
5.2.5	45 mm Bearing Operating Temperatures Vs. Axial Preload . . . .	24
5.2.6	45 mm Bearing Operating Temperatures Vs. Axial Preload . . . .	25
5.2.7	45 mm Bearing Operating Temperatures Vs. Friction Factor . . . .	27
5.2.8	45 mm Bearing Operating Temperatures Vs. Friction Factor . . . .	28
5.2.9	45 mm Bearing Operating Temperatures Vs. Friction Factor . . . .	29
5.2.10	45 mm Bearing Operating Temperatures Vs. Friction Factor . . . .	30
5.2.11	45 mm Bearing Operating Temperatures Vs. Friction Factor . . . .	31
5.2.12	45 mm Bearing Operating Temperatures Vs. Friction Factor . . . .	32
5.2.13	45 mm Bearing Operating Temperatures Vs. Heat Transfer Coeff..	33
5.2.14	45 mm Bearing Operating Temperatures Vs. Heat Transfer Coeff..	34
5.2.15	45 mm Bearing Operating Temperatures Vs. Heat Transfer Coeff..	35
5.2.16	45 mm Bearing Operating Temperatures Vs. Coolant Flow Rate . .	37
5.2.17	45 mm Bearing Operating Temperatures Vs. Coolant Flow Rate . .	38
5.2.18	45 mm Bearing Operating Temperatures Vs. Coolant Flow Rate . .	39
5.2.19	45 mm Bearing Operating Temperatures Vs. Inlet Coolant Flow Rate. . . . .	40
5.2.20	45 mm Bearing Operating Temperatures Vs. Inlet Coolant Flow Rate. . . . .	41
5.2.21	45 mm Bearing Operating Temperatures Vs. Inlet Coolant Flow Rate. . . . .	42
5.2.22	45 mm Bearing Operating Temperatures Vs. Inlet Coolant Flow Rate. . . . .	43
5.2.23	45 mm Bearing Operating Temperatures Vs. Inlet Coolant Rate. .	44
5.2.24	45 mm Bearing Operating Temperatures Vs. Outer Race Misalignment . . . . .	45
5.2.25	Outer Race to Isolator Clearance Vs. Component Temperatures. .	48
5.2.26	Fluid Quality Through Bearing #2 . . . . .	50
5.2.27	Fluid Quality Through Bearing #2 . . . . .	51

LIST OF TABLES

TABLE NUMBER		PAGE
5.1.1	Bearing Operating Characteristics with Uniform Temp. Profile .	14
5.1.2	Bearing Operating Characteristics Considering Thermal Effects.	14
5.2.1	Component Temperatures for Different Inlet Coolant Temperature at Low Flow Rate (3.6 lbs/sec) . . . . .	16
5.2.2	Component Temperatures for Different Inlet Coolant Temperature at High Flow Rate (7.0 lbs/sec). . . . .	17
5.2.3	Component Temperatures for Different Contact Friction Factors with 245% Increase in Heat Transfer Coefficient. . . . .	18
5.2.4	Component Temperatures for Different Contact Friction Factors with 343% Increase in Heat Transfer Coefficient. . . . .	19
5.2.5	Effect of Outer Race to Isolator Clearances. . . . .	47
5.2.6	Effects of Thermal Isolation of Bearing Isolator (45 mm Bearing) . . . . .	49

1.0 INTRODUCTION

This report describes the work accomplished under the Space Shuttle Main Engine (SSME) LOX Turbopump Bearing Analysis effort. The objectives of this activity were to model the SSME LOX turbopump bearings and shaft, and to evaluate the sensitivity of the pump-end bearing thermal and operating characteristics to a broad range of imposed conditions.

# *SRS Technologies*

## 2.0 SUMMARY

A simulation of the shaft/bearing system of the SSME LOX turbopump has been developed. The simulation model allows the thermal and mechanical characteristics to interact allowing a realistic simulation of the bearing operating characteristics. The model was used to investigate the sensitivity of bearing operating characteristics to variations in parameters such as contact friction, preloads, heat transfer coefficients, coolant flow, etc. Development of the system model involved two major modeling efforts; a pump shaft/bearing modeled on the SHABERTH computer code, and a detailed nodal model of the 45 mm pump bearing modeled on the SINDA thermal code. The SHABERTH model includes the shaft, pump-end bearing, and turbine-end bearing pairs. The inboard (Number 2) pump bearing is modeled in detail to allow determination of component temperature profiles and average temperatures. The model accounts for single- and two-phase coolant conditions, and includes the heat generation from bearing friction and fluid stirring. An executive program controls the iteration between the mechanical and thermal models to arrive at solutions satisfying both models. Solutions that satisfy both models are considered to be realistic and are designated as converged solutions. When the models are not simultaneously satisfied, the solution diverges and a realistic operating condition is assumed not to exist.

Using the simulation model, parametric analyses were performed on the 45 mm pump-end bearing to investigate the sensitivity of bearing characteristics to contact friction, axial preload, coolant flow rate, coolant inlet temperature and quality, heat transfer coefficients, outer race clearance and misalignment, and the effects of thermally isolating the outer race from the isolator. The shaft speed was 30,000 RPM and a radial load profile was used that produced reactions measured in pump build 2606 R1.

Bearing component temperatures (average and peak) were found to be very sensitive to contact friction, axial preload, and boundary heat transfer conductance. The effects of coolant flow rate and inlet conditions (temperature and quality) are not as dramatic. However, at the more severe conditions (i.e., high friction and loads, they can be an important factor in determining the thermal stability of the shaft/bearing system. The effect on component temperatures of varying outer race-to-isolator clearance is small,

## *SRS Technologies*

over the range of clearance investigated. Outer race clearance was lost, for the Number 2 bearing, for the majority of the cases investigated. Since the analysis only considered radial loads, the consequence of the loss in outer race clearance was not fully determined. The loss of clearance could prevent axial movement of the outer race, with resultant high axial loads especially during engine power level changes.

A maximum surface temperature of about 1800°F was estimated for the most severe case that converged. This case involved an outer race misalignment of ~29 minutes. The highest surface temperature with perfect outer race alignment was ~700°F. The large increases in temperature with small errors in outer race alignment show how critical proper installation of the outer race is to bearing operation.

Load sharing of the Number 1 and 2 pump bearings is not equal. Initially this is primarily due to shaft deflection which transmits more of the radial load to the Number 2 bearing. Due to the heavier load, the Number 2 bearing heats up, loses internal clearance, and becomes stiffer in the radial direction than the Number 1 bearing. This causes the Number 2 bearing to share an even greater part of the load with increasing temperatures and further loss of internal clearance. Analysis indicates that an internal clearance of at least 3.9 mils is necessary to maintain thermal stability for the conditions evaluated. If conditions (load, friction, etc.) become too severe, the bearing can experience severe thermal distress which can lead to failure.

Discoloration of bearing components indicates surface temperature in excess of the ~700°F maximum predicted for stable operating conditions. There are two possible reasons for these differences in hardware observations and model predictions. The high temperatures indicated by the hardware could result from transient excursions which do not dwell long enough for the system to become thermally unstable. These conditions could produce high surface temperatures, but not dwell long enough for the average temperature to increase sufficiently to lose critical internal clearance. Ball milling or rapid ball wear experienced with the 45 mm bearing in effect increases the internal clearance, and could allow the bearing to survive when it would otherwise fail due to over temperature and loss of critical internal clearance.



# *SRS Technologies*

## 3.0 SHAFT/BEARING MODEL DESCRIPTION

A shaft/bearing system model was developed to represent the Space Shuttle Main Engine (SSME) Liquid Oxygen (LOX) turbopump shaft and bearing configuration using the SHABERTH computer program. A thermal model was developed specifically for the 45 mm pump-end bearing using the Systems Improved Numerical Differencing Analyzer (SINDA) program.

### 3.1 SHABERTH Shaft/Bearing Model

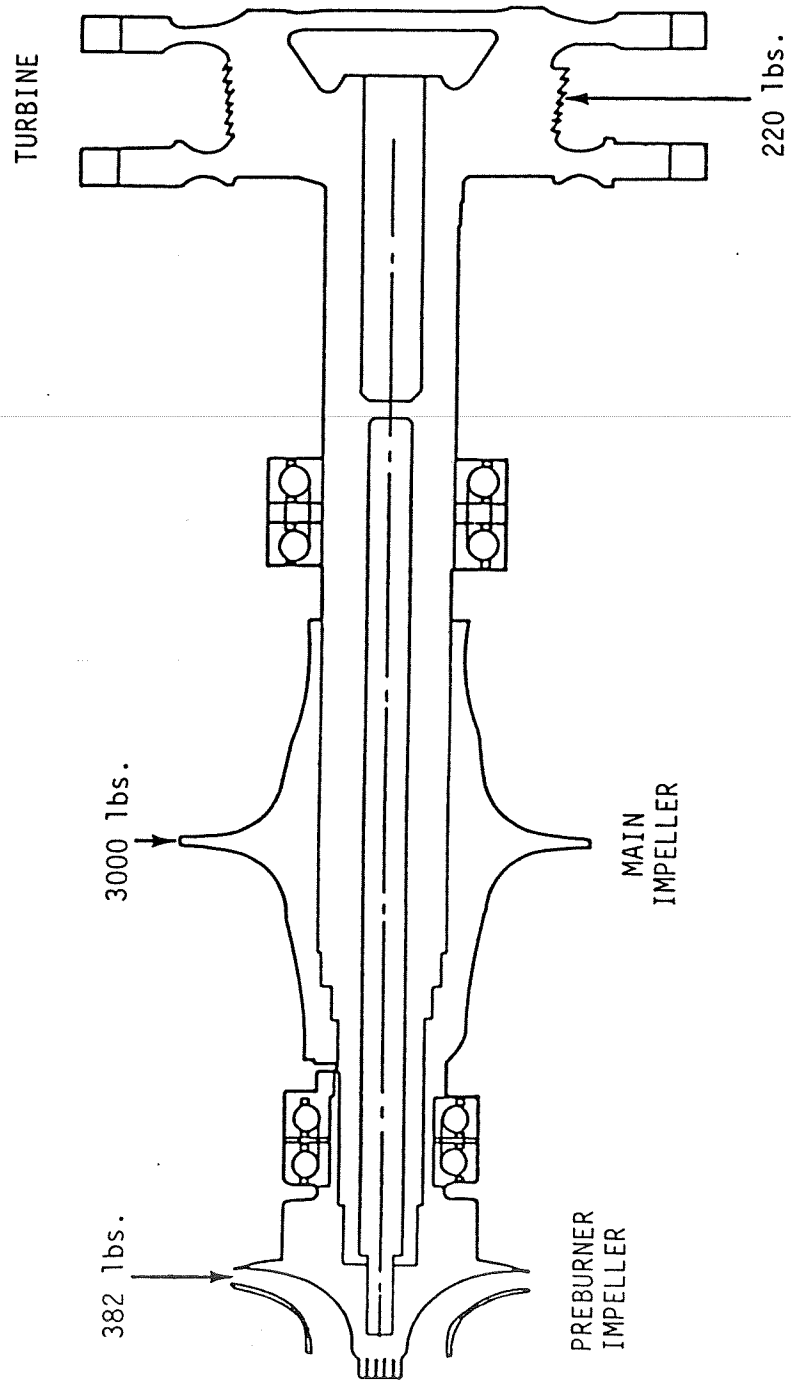
The SHABERTH model for the SSME LOX turbopump consists of the turbopump shaft, turbine-end and pump-end bearings. The major components of the shaft/bearing model are shown in Figure 3.1.1. The complete shaft/bearing system was modeled so that the effects of preload and shaft deflection on bearing load sharing could be studied. Variations in outer race clearance, outer race tilt, and contact friction could also be investigated using this model. The model used a shaft speed of 30,000 RPM and shaft loading conditions presented in Figure 3.1.1. These radial loads were used to produce the reactions reported for pump build number 2606R1. The SHABERTH model predicts the frictional heat generation at the contact points in the bearing and the load distribution for each bearing set.

### 3.2 SINDA Thermal Model of 45 mm Bearing

The SINDA thermal model is a detailed nodal division of the SSME LOX turbopump Number 2 bearing. The SINDA thermal model, using the nodal representation of the bearing components (inner race, ball, outer race, etc.), is able to predict component temperature profiles and average component temperatures. The thermal model uses the energy conservation equation to obtain the temperature distribution in the bearing components. The model solves the conservation equation using the bearing frictional heat generation, predicted by the SHABERTH model, and fluid stirring heat generation. The thermal model also accounts for the heat generated by pump-end bearing Number 1.

The SINDA thermal model is able to simulate different coolant flow rates and inlet coolant temperatures. The model is capable of simulating saturated coolant entering bearing Number 2. Also, thermal isolation of specific components in the bearing can be performed with this model.

FIGURE 3.1.1.1 SSME LOX TURBOPUMP BEARING/SHAFT LOAD CONFIGURATION



# *SRS Technologies*

## 3.3 Model Iteration Process

The SHABERTH shaft/bearing model and the SINDA thermal model are used in an interactive iteration process to determine the steady state operating conditions for a specific case. The iteration process can also predict if a case is thermally unstable.

The iteration process is totally automated. The user supplies an initial guess for the bearing component temperatures and the models iterate until a solution is determined. The models are first set up to simulate a specific case. The user then supplies an initial guess for the component temperatures to the SHABERTH shaft/bearing model. The SHABERTH model then analyses the shaft/bearing system and calculates the frictional heat generation rates of the contact points in the bearing. These heat generation rates are placed in the SINDA thermal model. SINDA then solves the energy conservation equation to predict the temperature distribution in the bearing components. The average component temperatures are calculated from the temperature profiles and are used in a comparison with the average component temperatures used by the SHABERTH model. If all the temperatures compare to within 2°C, the steady state solution has been reached. If the comparison fails, the SHABERTH model uses the new temperatures to predict new frictional heat rates. The thermal model uses the new heat rates to predict another set of average component temperatures. The temperature comparison is again made.

The iteration process is continued in this manner until the temperatures used by the SHABERTH model are within 2°C of the temperatures predicted by the thermal model or the predicted temperatures exceed an upper limit of 2000°F. 2000°F was chosen as the approximate ignition temperature of 440C in liquid oxygen. A case is considered thermally unstable if an average component temperature exceeds the 2000°F limit. Figure 3.3.1 illustrates the iteration process between the SHABERTH shaft/bearing model and the SINDA thermal model for a converged case. In this case the friction heat from SHABERTH and the average component temperature from SINDA increase to a converged point. Figure 3.3.2 shows a diverged (thermally unstable) case which has no converged point.

FIGURE 3.3.1 ITERATION PROCESS BETWEEN SHABERTH AND SINDA

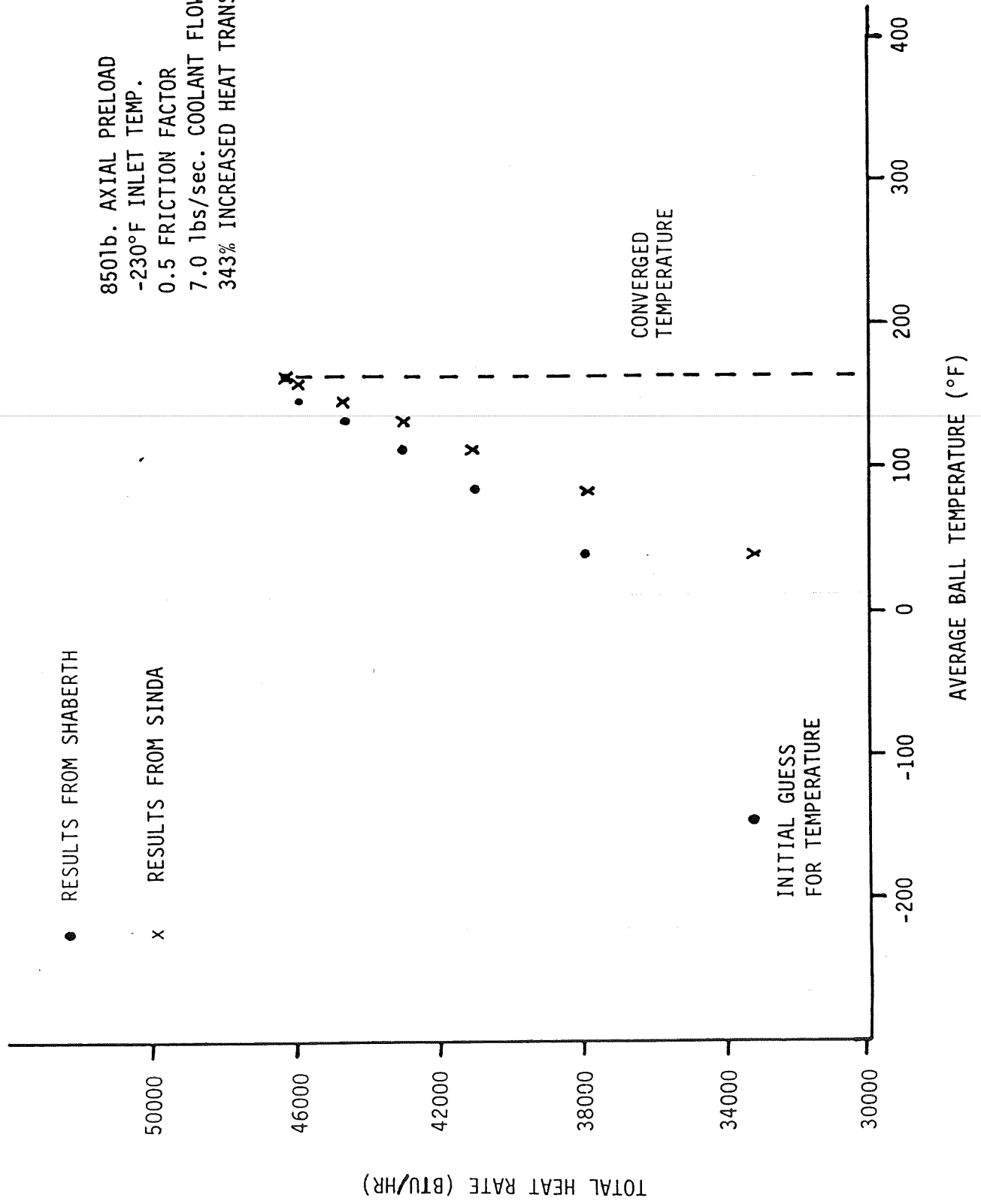
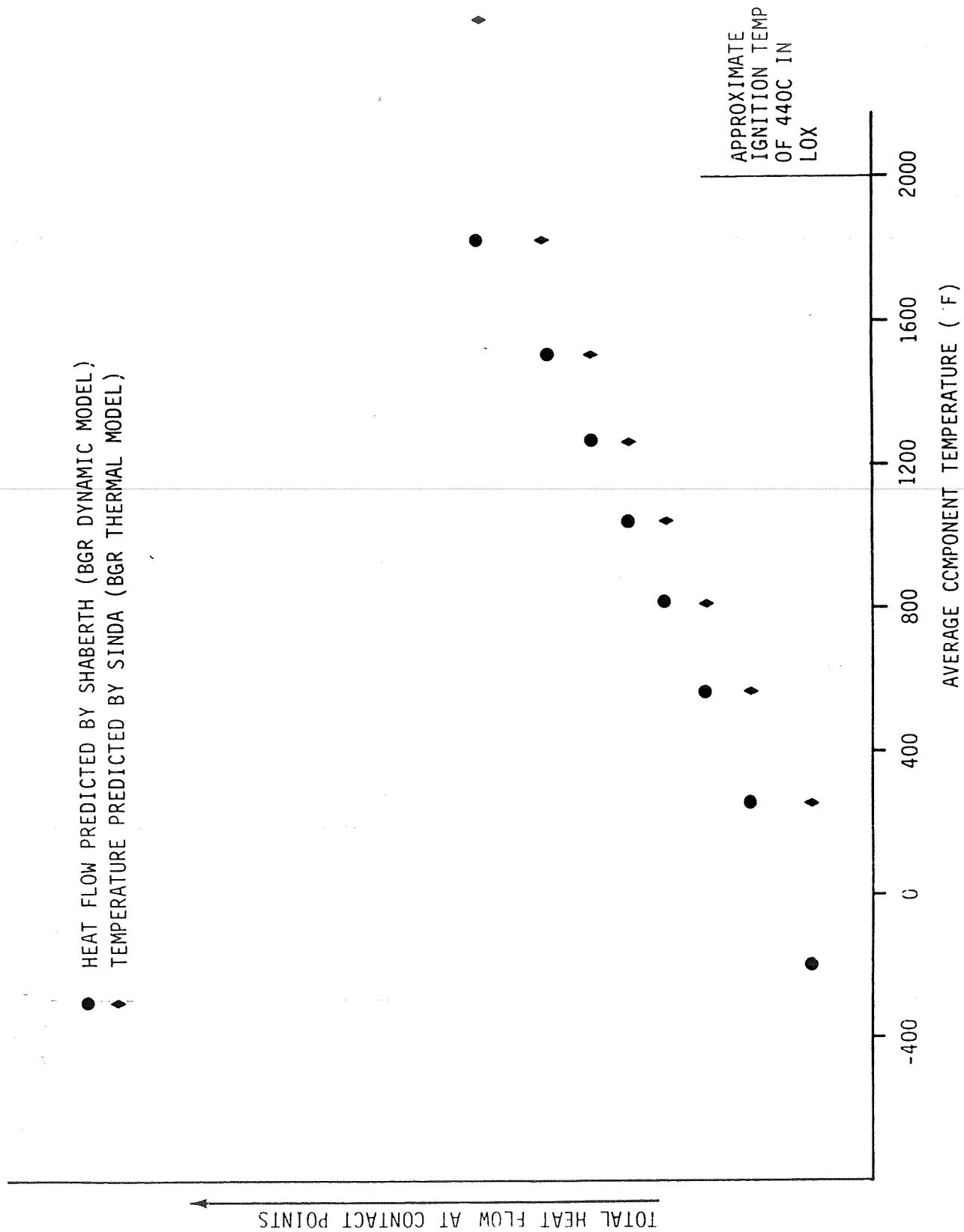


FIGURE 3.3.2 EXAMPLE OF A DIVERGED ITERATION PROCESS  
(DIVERGED CASE)



# SRS Technologies

## 4.0 ANALYSIS OBJECTIVES AND APPROACH

The objectives of the SSME LOX turbopump pump-end bearing analysis were to investigate the sensitivity of bearing operating characteristics to variations in operating parameters. The operating parameters that were considered are listed below with the values investigated.

1. Coolant Flow Rate (lbs/sec)	3.6, 7.0
2. Contact Friction Factor	0.2, 0.3, 0.5
3. Inlet Coolant Temperature to Bearing #1 (°F)	-240, -230, -218
4. Axial Preload (lbs)	350, 480, 850
5. Outer Race Clearance (mils)	2.6, 1.7, 1.0
6. Outer Race Tilt (minutes)	0 through 42
7. Heat Transfer Between Outer Race and Isolator	With, Without

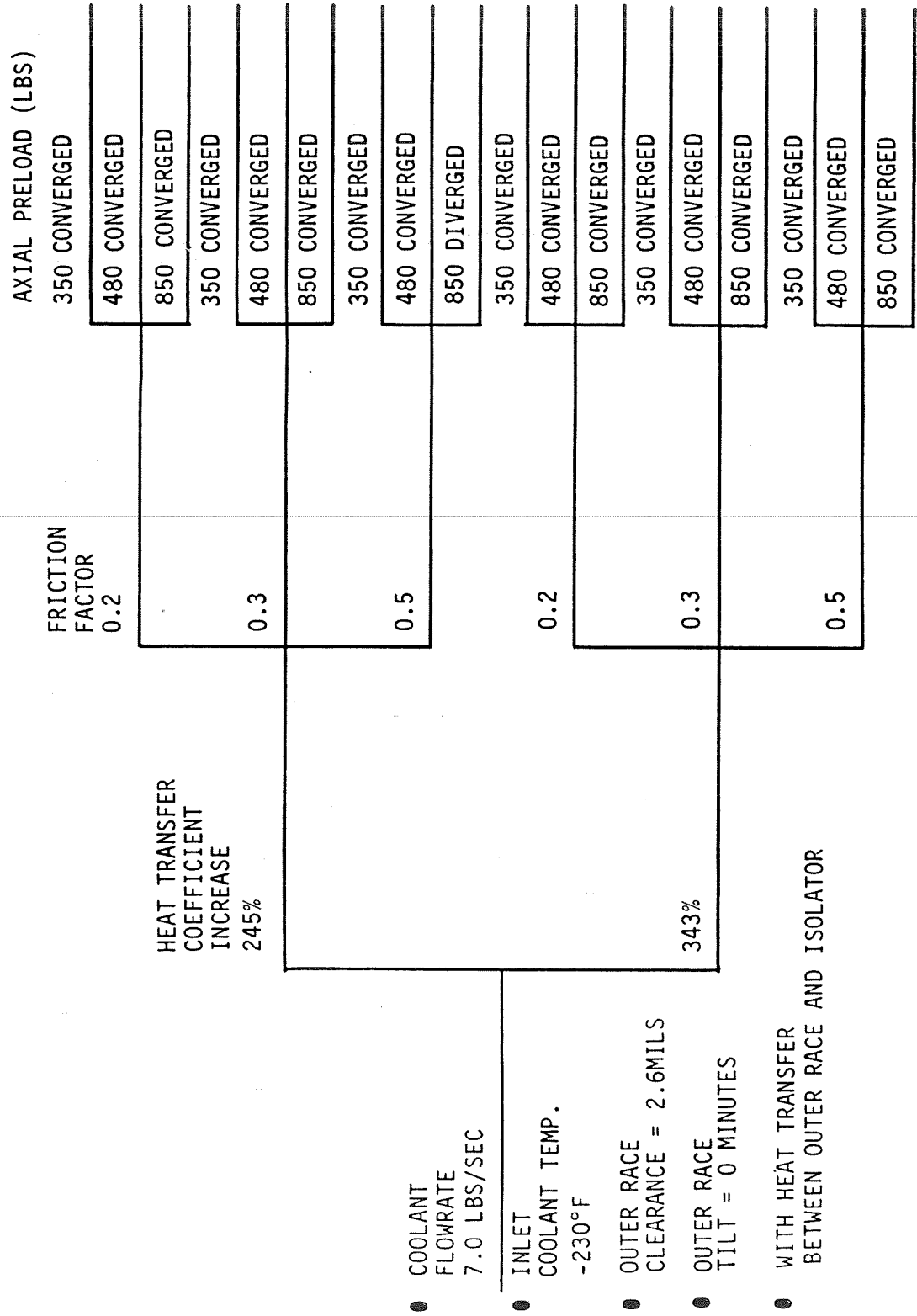
The flow rate, friction factor, inlet temperature, and preload were investigated in all combinations while holding the remaining parameters at their initial values. This resulted in 54 initial cases to be simulated. These cases are represented in the parameter data tree of Figure 4.1. This figure shows that 42 of the 54 cases were thermally unstable (diverged). It was not necessary to run computer simulations for all the cases to determine thermal instability. For example, if a case with an inlet coolant temperature of -218°F, flow rate of 7.0 lbs/sec, preload of 850 lbs, and friction factor of 0.2 was unstable, then cases for friction factor of 0.3 and 0.5 with the other parameters the same would obviously not be stable.

The effect of changes in coolant flow rate and inlet coolant temperature were evaluated using the 12 converged cases. However, more converged cases, over the full range of parameter values, were needed to properly evaluate changes in the remaining operating parameters. Thus, it was decided to increase the boundary heat transfer coefficient to obtain more cases that are thermally stable.

Changing the boundary heat transfer coefficient introduced heat transfer as a new parameter into the sensitivity analysis. A second parameter data tree was developed for the increased heat transfer coefficients and unevaluated parameters. Figure 4.2 shows this parameter data tree, which has 18



FIGURE 4.2 PARAMETER DATA TREE WITH ENHANCED HEAT TRANSFER COEFFICIENT





## *SRS Technologies*

more cases. The effect of varying friction factor and axial preload were properly evaluated using these cases.

The heat transfer coefficient was increased to obtain converged cases over the range of parameter values. A thermally stable solution was obtained for a coolant flow rate of 7.0 lbs/sec, inlet temperature of -230°F, friction factor of 0.5, and preload of 480 lbs with a 245 percent increase in heat transfer coefficient. An increase in heat transfer coefficient of 343 percent was needed for the 850 lb preloaded case.

The variation of outer race clearance, outer race tilt, and thermal isolation of the isolator were evaluated separately, holding all other parameters constant. A nominal case with a flow rate of 7.0 lbs/sec, inlet temperature of -230°F, friction factor of 0.2, and preload of 480 lbs was used to evaluate these parameters. The 245 percent increased heat transfer coefficient was needed for the evaluation of outer race clearance changes. The 343 percent increased heat transfer coefficient was needed to evaluate the effects of changing outer race tilt.

## 5.0 ANALYSIS RESULTS

The analysis of the SSME LOX turbopump included different loading conditions and bearing temperature profiles. A mechanical analysis of the shaft/bearing system was performed using the SHABERTH computer model. The thermal analysis of the pump-end Number 2 (inboard) bearing was performed using the SINDA thermal model. The use of these computer models, in an interactive manner, enabled the comprehensive evaluation of the bearing performance.

### 5.1 Mechanical Characteristics

The mechanical analysis was performed using a shaft speed of 30,000 RPM and radial loads on the preburner impeller, main impeller, and turbine of 382, 3000, and -220 lbs, respectively. These radial loads, illustrated in Figure 3.1.1, were used to produce the reaction loads measured for pump build 2606R1. The model used an unmounted diametrical clearance of 6.3 mils, inner race curvature of 0.55, and outer race curvature of 0.52 for the 45 mm inboard (Number 2) bearing. The model also simulates the outer races sliding with axial load. This was done by manipulating the turbine-end bearings so that they transmit very small axial loads to the pump-end bearings.

The bearing operating characteristics were determined for a case using 480 lbs preload, 7.0 lbs/sec coolant flow rate, and friction factor of 0.2. Table 5.1.1 shows the bearing operating characteristics for a uniform temperature profile of -230°F. Table 5.1.2 shows the same case at its steady state (converged) temperature profile. As can be seen from these tables, the pump-end bearings (Numbers 1 and 2) do not share an equal amount of the load. This is primarily due to the shaft deflecting from the large radial load placed between the pump-end bearings and the turbine-end bearings (Numbers 3 and 4). Bearing 2 received about 72 percent of the load to the pump-end bearings with a uniform temperature profile. The bearing received about 76 percent of the load, considering thermal effects. Bearing 2 received a greater portion of the load with the steady state temperature profile because of thermal growth of the ball, with respect to the races. The thermal growth of the ball decreased the internal clearances in the bearing which increased the axial load. The increased axial load caused the bearing to become "stiffer" and able to support a larger radial load.

TABLE 5.1.1 BEARING OPERATING CHARACTERISTICS  
WITH UNIFORM TEMP. PROFILE

BEARING NO.	REACTION FORCES(lbs)		MOMENTS (ft/lbs)	MAX. HERTZ STRESSES (kpsi)	DEFLECTIONS (inches)
	RADIAL	AXIAL			
1	618.7	941.5	-32.2	377	0.00080
2	1572	-1042	84.8	469	0.00114
3	1292	114.3	-10.0	382	0.00053
4	-320.8	-14.32	-3.55	300	-0.00014

480 LBS AXIAL PRELOAD  
6.3 MILS DIAMETRICAL CLEARANCE  
2.6 MILS OUTER RACE CLEARANCE

TABLE 5.1.2 BEARING OPERATING CHARACTERISTICS  
CONSIDERING THERMAL EFFECTS

BEARING NO.	REACTION FORCES(lbs)		MOMENTS (ft/lbs)	MAX. HERTZ STRESSES (kpsi)	DEFLECTIONS (inches)
	RADIAL	AXIAL			
1	530.8	1040	-26.6	374	0.00074
2	1650	-1170	88.6	486	0.00116
3	1495	145.4	-12.9	402	0.00058
4	-513.5	-15.13	-4.76	327	0.00021

480 LBS AXIAL PRELOAD  
6.3 MILS DIAMETRICAL CLEARANCE  
2.6 MILS OUTER RACE CLEARANCE

# *SRS Technologies*

## 5.2 Thermal Analysis Results

The SINDA thermal model predicted temperatures for each node of the bearing components. The program then calculates the volume average temperature for the main components. Tables 5.2.1 through 5.2.4 show the average component and maximum track temperatures for the cases studying preload, friction factor, inlet temperature, and flow rate.

The calculated results with nominal heat transfer coefficient are shown in Table 5.2.1 and 5.2.2. The effect of preload and inlet coolant temperatures are shown for a friction factor of 0.2 with two flow rates considered. No stable solution was achieved for 850 lbs preload. Therefore, it was necessary to increase the heat transfer coefficient to obtain more stable cases. Table 5.2.3 presents the results for three friction factors and three preloads for cases where the heat transfer coefficient has been increased to 245% of its nominal value. With this increase, it was possible to obtain a thermally stable solution for all cases except the case with 0.5 friction factor and 850 lbs preload. To obtain a thermally stable solution for this case, the heat transfer coefficient was increased by 343%. The results of the cases studied with 343% increase in heat transfer coefficient have been reported in Table 5.2.4. The maximum track temperature has been found to be 719°F with a friction factor of 0.5 and a preload of 850 lbs. It should be observed that the higher track temperatures for stable cases occur with the higher heat transfer coefficients and friction coefficients. These conditions allow high local heating while providing the capability to remove sufficient heat to prevent thermal instability.

### Effect of Axial Preload

The effect of varying axial preload on the 45 mm inboard bearing was determined for friction factors of 0.2, 0.3, and 0.5. Figures 5.2.1 through 5.2.3 show the effect of axial preload using the increased heat transfer coefficient of 245%. Figures 5.2.4 through 5.2.6 show the effect of preload using the 343% increased heat transfer coefficient. The figures show that axial preload does have a significant effect on operating temperatures. The effect of preload is increased as the friction factor is increased. At a friction factor of 0.2, the average ball temperature increases by 31°F with

TABLE 5.2.1 COMPONENT TEMPERATURES FOR DIFFERENT INLET COOLANT TEMPERATURES AT LOW FLOW RATE (3.6 LBS/SEC)

45 MM BEARING

INLET COOLANT TEMPERATURE		BEARING AXIAL PRELOAD (LBS)																	
		350				480				850									
BEARING 1	BEARING 2	AVERAGE TEMPERATURE (°F)			MAXIMUM TRACK TEMPERATURE (°F)			AVERAGE TEMPERATURE (°F)			MAXIMUM TRACK TEMPERATURE (°F)			AVERAGE TEMPERATURE (°F)			MAXIMUM TRACK TEMPERATURE (°F)		
		INNER RACE	BALL	OUTER RACE	INNER RACE	BALL	OUTER RACE	INNER RACE	BALL	OUTER RACE	INNER RACE	BALL	OUTER RACE	INNER RACE	BALL	OUTER RACE	INNER RACE	BALL	OUTER RACE
-240	-232	-144	-23	-125	65	89	102	-106	47	-101	159	182	172	*	*	*	*	*	*
-230	-223	-125	-1	-113	93	115	120	-95	57	-95	177	195	169	*	*	*	*	*	*
-218	-214	-113	8	-105	106	124	128	-88	63	-88	185	200	176	*	*	*	*	*	*

COOLANT FLOWRATE = 3.6 LBS/SEC

FRICTION FACTOR = 0.2

\* THERMALLY UNSTABLE

TABLE 5.2.2 COMPONENT TEMPERATURES FOR DIFFERENT INLET  
COOLANT TEMPERATURES AT HIGH FLOW RATE (7.0 LBS/SEC)

45 MM BEARING

INLET COOLANT TEMPERATURE		BEARING AXIAL PRELOAD (LBS)																	
		350				480				850									
		AVERAGE TEMPERATURE (°F)		MAXIMUM TRACK TEMPERATURE (°F)		AVERAGE TEMPERATURE (°F)		MAXIMUM TRACK TEMPERATURE (°F)		AVERAGE TEMPERATURE (°F)		MAXIMUM TRACK TEMPERATURE (°F)							
BEARING 1	BEARING 2	INNER RACE	BALL	OUTER RACE	INNER RACE	BALL	OUTER RACE	INNER RACE	BALL	OUTER RACE	INNER RACE	BALL	OUTER RACE						
-240	-236	-151	-32	-132	5	79	94	-130	11	-119	118	139	127	*	*	*	*	*	*
-230	-226	-130	-8	-118	85	107	114	-102	49	-101	167	185	162	*	*	*	*	*	*
-218	-214	-113	8	-105	106	124	128	-86	66	-87	188	204	178	*	*	*	*	*	*

COOLANT FLOWRATE = 7.0 LBS/SEC

FRICTION FACTOR = 0.2

\* THERMALLY UNSTABLE

TABLE 5.2.3 COMPONENT TEMPERATURES FOR DIFFERENT CONTACT FRICTION FACTORS WITH 245% INCREASE IN HEAT TRANSFER COEFFICIENT

45 MM BEARING

FRICTION FACTOR	BEARING AXIAL PRELOAD (LBS)																	
	350				480				850									
	AVERAGE TEMPERATURE (°F)		MAXIMUM TRACK TEMPERATURE (°F)		AVERAGE TEMPERATURE (°F)		MAXIMUM TRACK TEMPERATURE (°F)		AVERAGE TEMPERATURE (°F)		MAXIMUM TRACK TEMPERATURE (°F)							
INNER RACE	BALL	OUTER RACE	INNER RACE	BALL	OUTER RACE	INNER RACE	BALL	OUTER RACE	INNER RACE	BALL	OUTER RACE	INNER RACE	BALL	OUTER RACE				
0.2	-197	-158	-173	-64	-67	-17	-193	-150	-171	-44	-50	-9	-179	-120	-160	24	8	27
0.3	-176	-110	-139	33	27	106	-164	-96	-133	74	59	123	123	-12	-100	240	205	220
0.5	-98	46	-38	330	307	426	-40	157	6	558	503	560	*	*	*	*	*	*

FLOWRATE = 7.0 LBS/SEC

INLET COOLANT TEMPERATURE = -230°F

INCREASE IN HEAT TRANSFER COEFFICIENT OF 245%

\* THERMALLY UNSTABLE

TABLE 5.2.4 COMPONENT TEMPERATURES FOR DIFFERENT CONTACT FRICTION FACTORS WITH 343% INCREASE IN HEAT TRANSFER COEFFICIENT

45 MM BEARING

FRICTION FACTOR	BEARING AXIAL PRELOAD (LBS)																	
	350				480				850									
	AVERAGE TEMPERATURE (°F)		MAXIMUM TRACK TEMPERATURE (°F)		AVERAGE TEMPERATURE (°F)		MAXIMUM TRACK TEMPERATURE (°F)		AVERAGE TEMPERATURE (°F)		MAXIMUM TRACK TEMPERATURE (°F)							
INNER RACE	BALL	OUTER RACE	INNER RACE	BALL	OUTER RACE	INNER RACE	BALL	OUTER RACE	INNER RACE	BALL	OUTER RACE	INNER RACE	BALL	OUTER RACE				
0.2	-209	-185	-188	-94	-104	-54	-206	-180	-186	-77	-90	-46	-193	-154	-176	-23	-42	-17
0.3	-191	-147	-159	-14	-26	51	-186	-138	-156	14	-4	64	-168	-102	-141	108	73	114
0.5	-149	-62	-92	185	156	292	-132	-32	-81	261	218	328	-28	164	11	719	597	618

FLOWRATE = 7.0 LBS/SEC  
 INLET COOLANT TEMPERATURE = -230 °F  
 INCREASE IN HEAT TRANSFER COEFFICIENT OF 343%



FIGURE 5.2.1 45mm BEARING OPERATING TEMP.  
VERSUS AXIAL PRELOAD

- 0.2 FRICTION FACTOR
- 7.0 LBS/SEC COOLANT FLOW
- -230 °F INLET COOLANT TEMPERATURE
- INCREASED HEAT TRANSFER COEFFICIENT (245%)

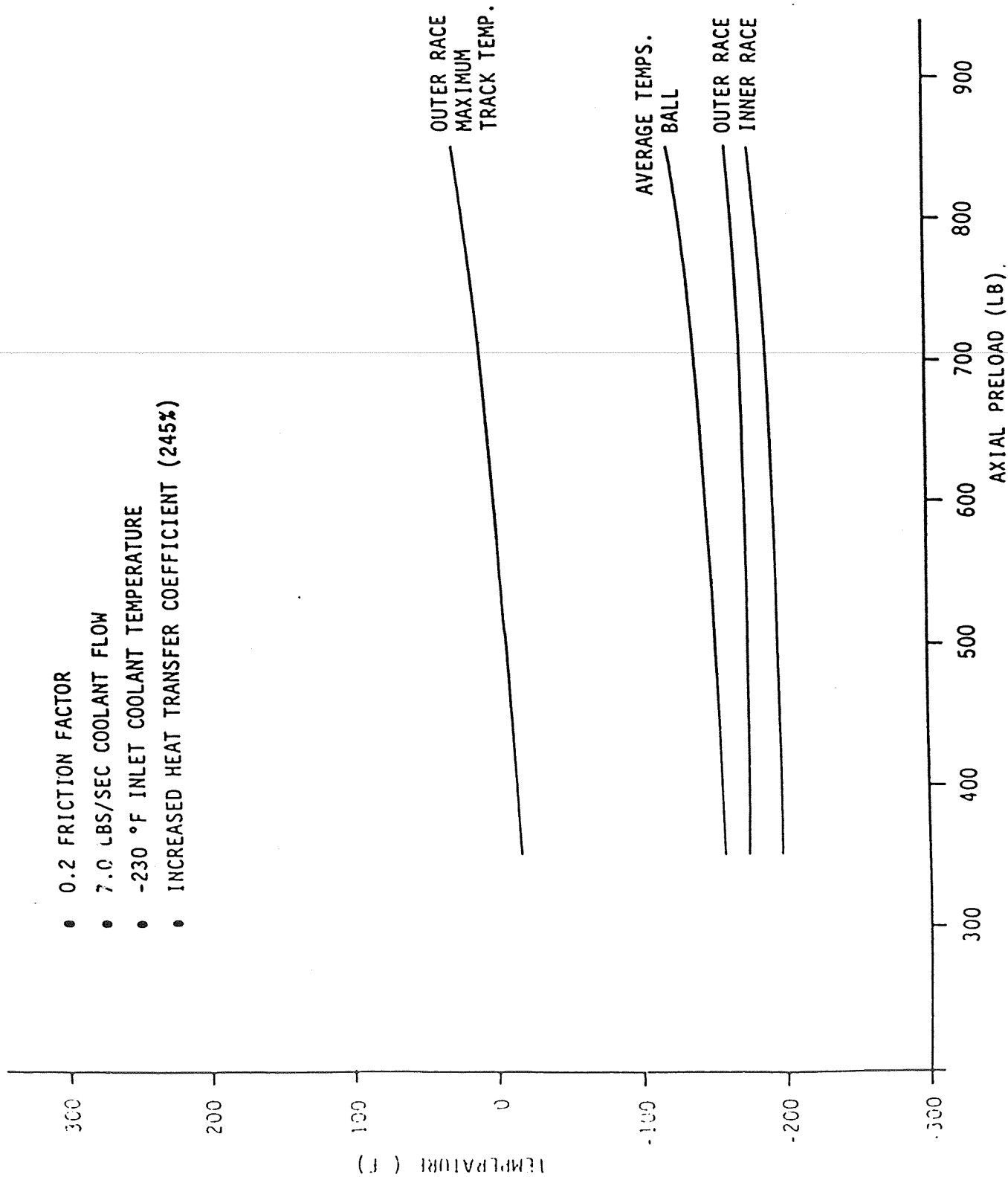


FIGURE 5.2.2 45mm PUMP END BEARING OPERATING TEMPERATURES VS. AXIAL PRELOAD

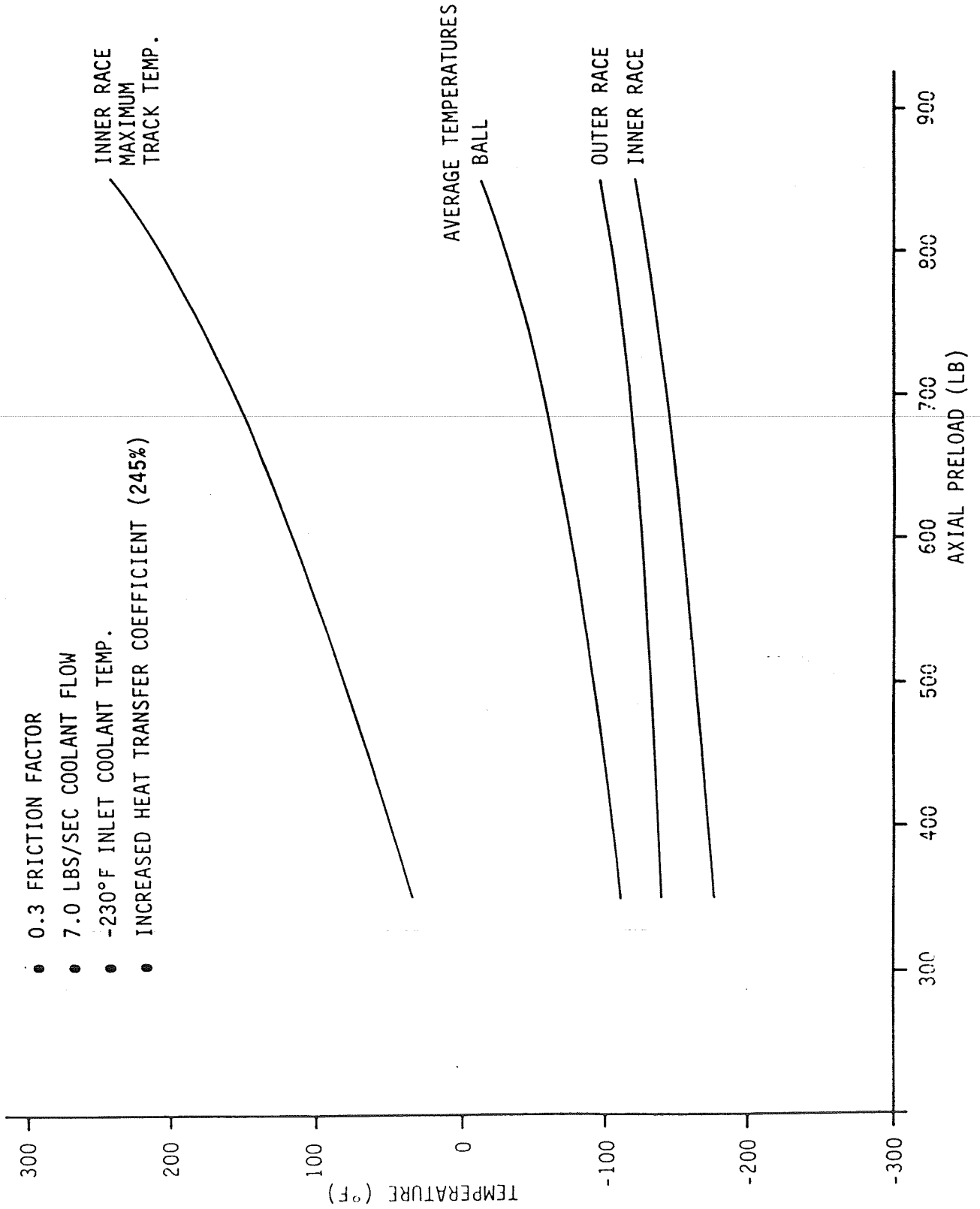


FIGURE 5.2.3 45mm BEARING OPERATING TEMPERATURES  
VS. AXIAL PRELOAD

- 0.5 FRICTION FACTOR
- 7.0 LBS/SEC COOLANT FLOW
- -230°F INLET COOLANT TEMPERATURE
- INCREASE HEAT TRANSFER COEFFICIENT (245%)

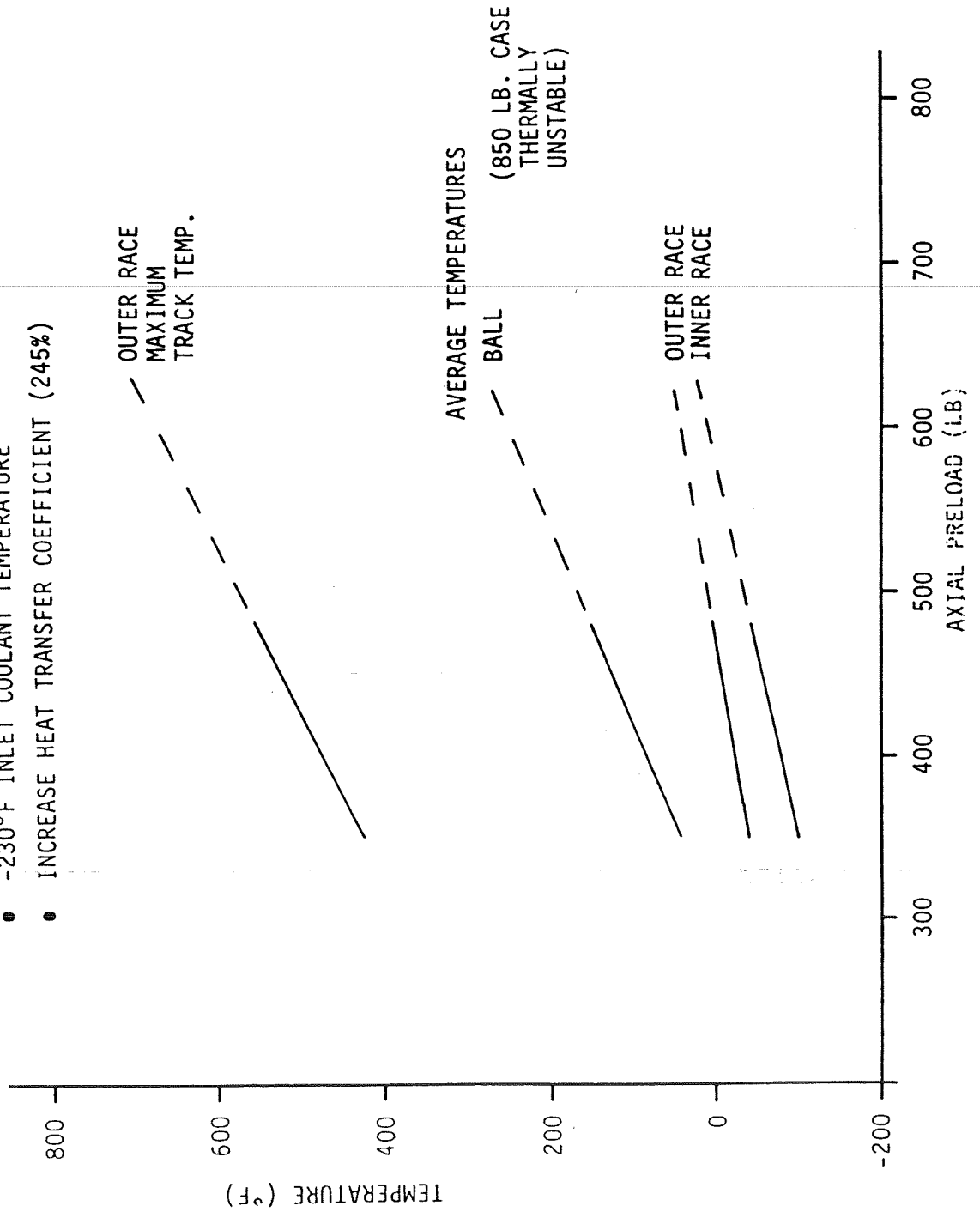


FIGURE 5.2.4 45mm BEARING OPERATING TEMP. VERSUS AXIAL PRELOAD

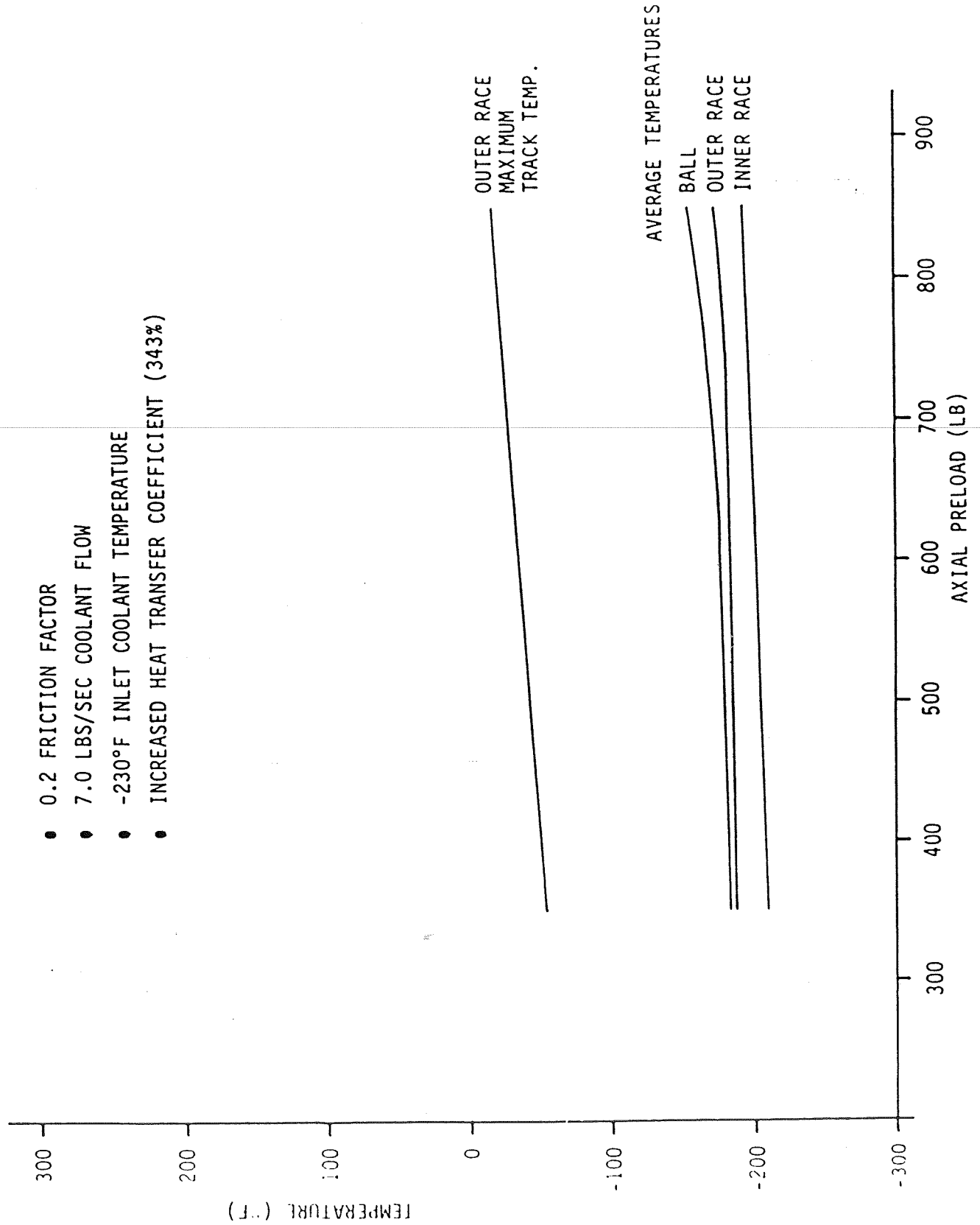


FIGURE 5.2.5 45mm BEARING OPERATING TEMPERATURES  
VS. AXIAL PRELOAD

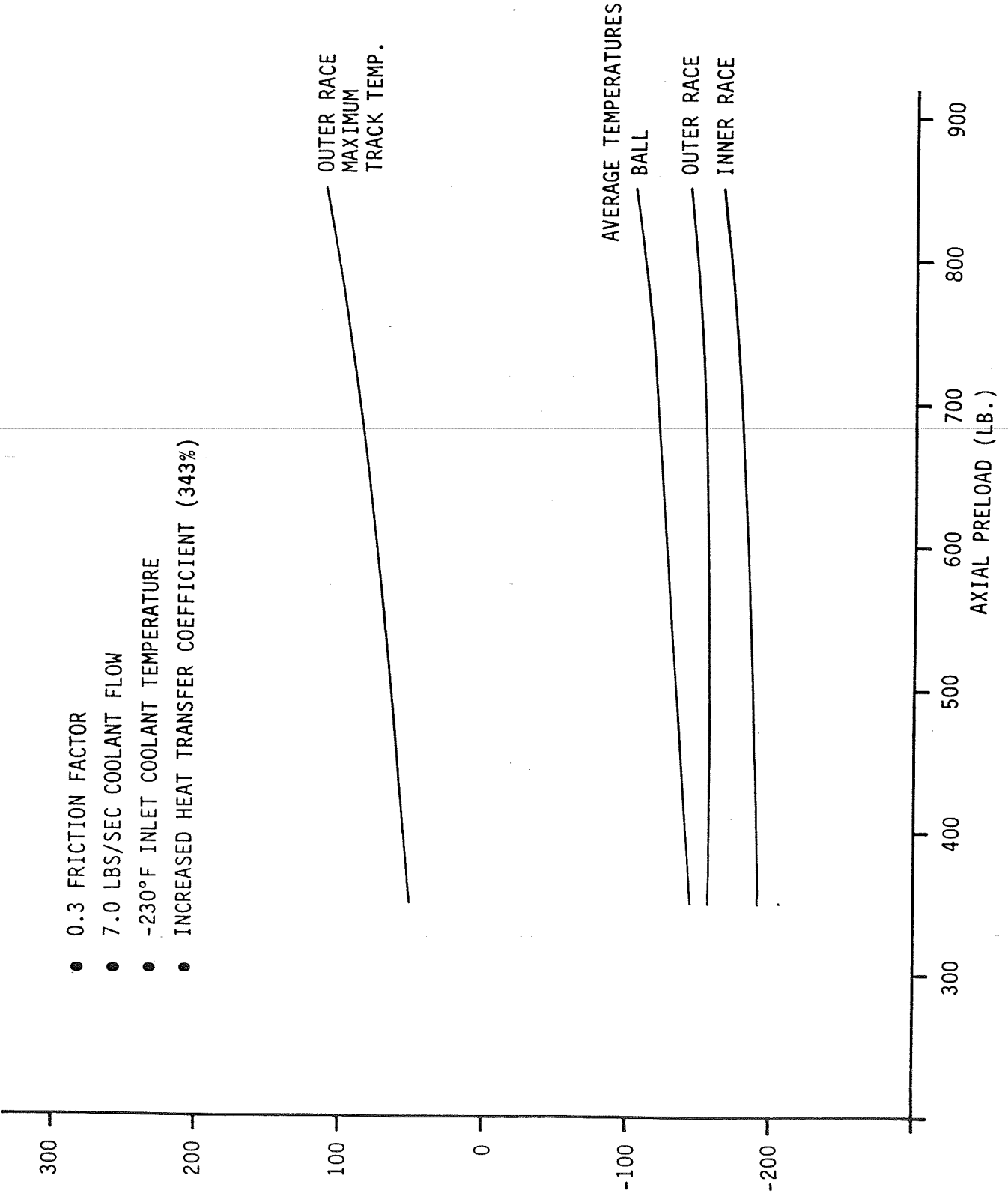
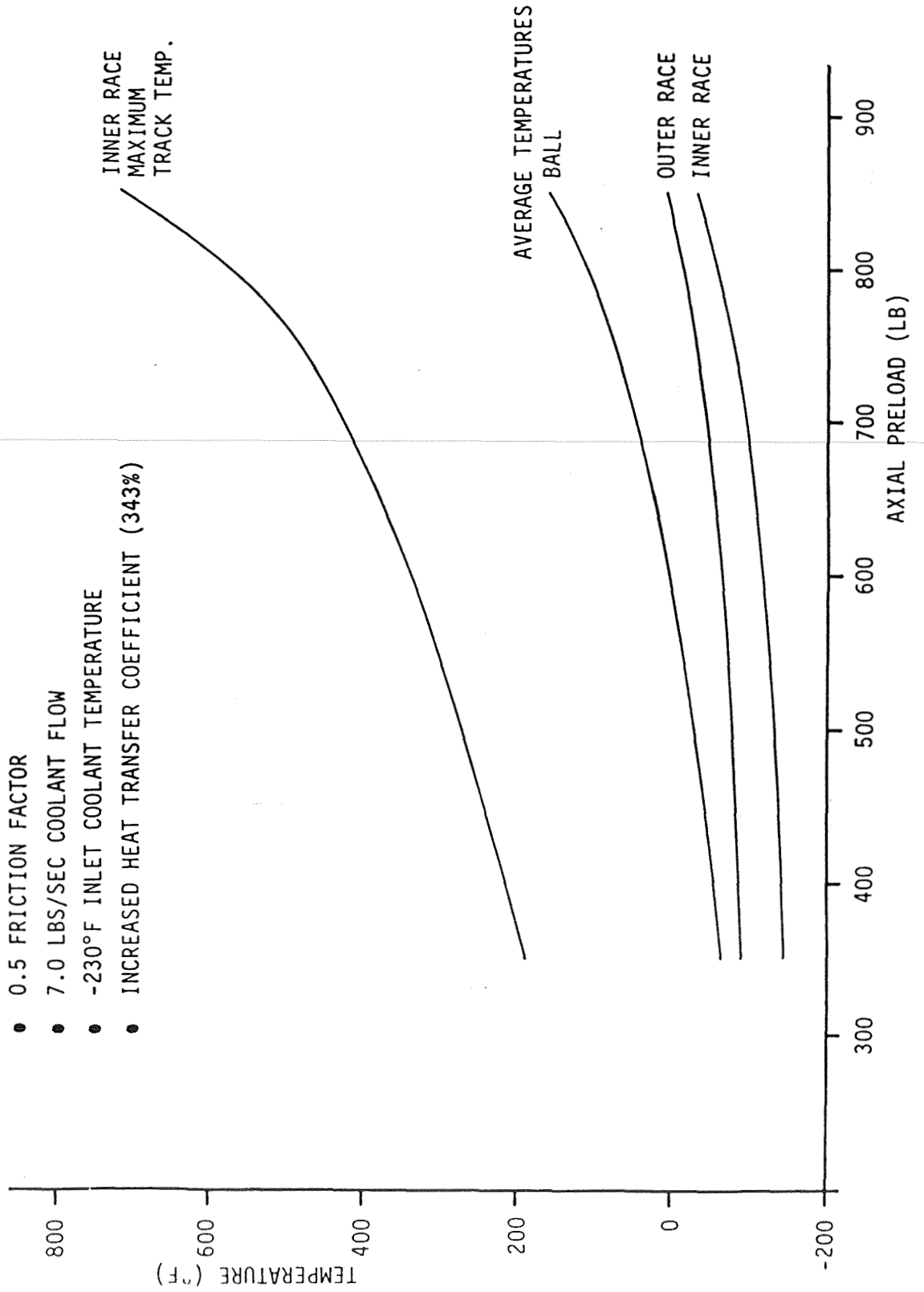


FIGURE 5.2.6 45mm BEARING OPERATING TEMPERATURES  
VS. AXIAL PRELOAD



## *SRS Technologies*

an increase of preload from 350 to 850 lbs. At a friction of 0.5, the average ball temperature increased by 226°F with an increase in preload from 350 to 850 lbs. The dashed line in Figure 5.2.3 indicates that the 850 lb preload case did not have a thermally stable solution.

### Effect of Friction Factor

The effect of increasing the friction factor for preloads of 350, 480, and 850 lbs and the two increased heat transfer coefficients are shown in Figures 5.2.7 through 5.2.12. The results show that contact friction has a large effect on bearing operating temperatures. An increase in friction factor from 0.2 to 0.5 increased the average ball temperature by 123°F for a preload of 350 lbs and 318°F with a preload of 850 lbs.

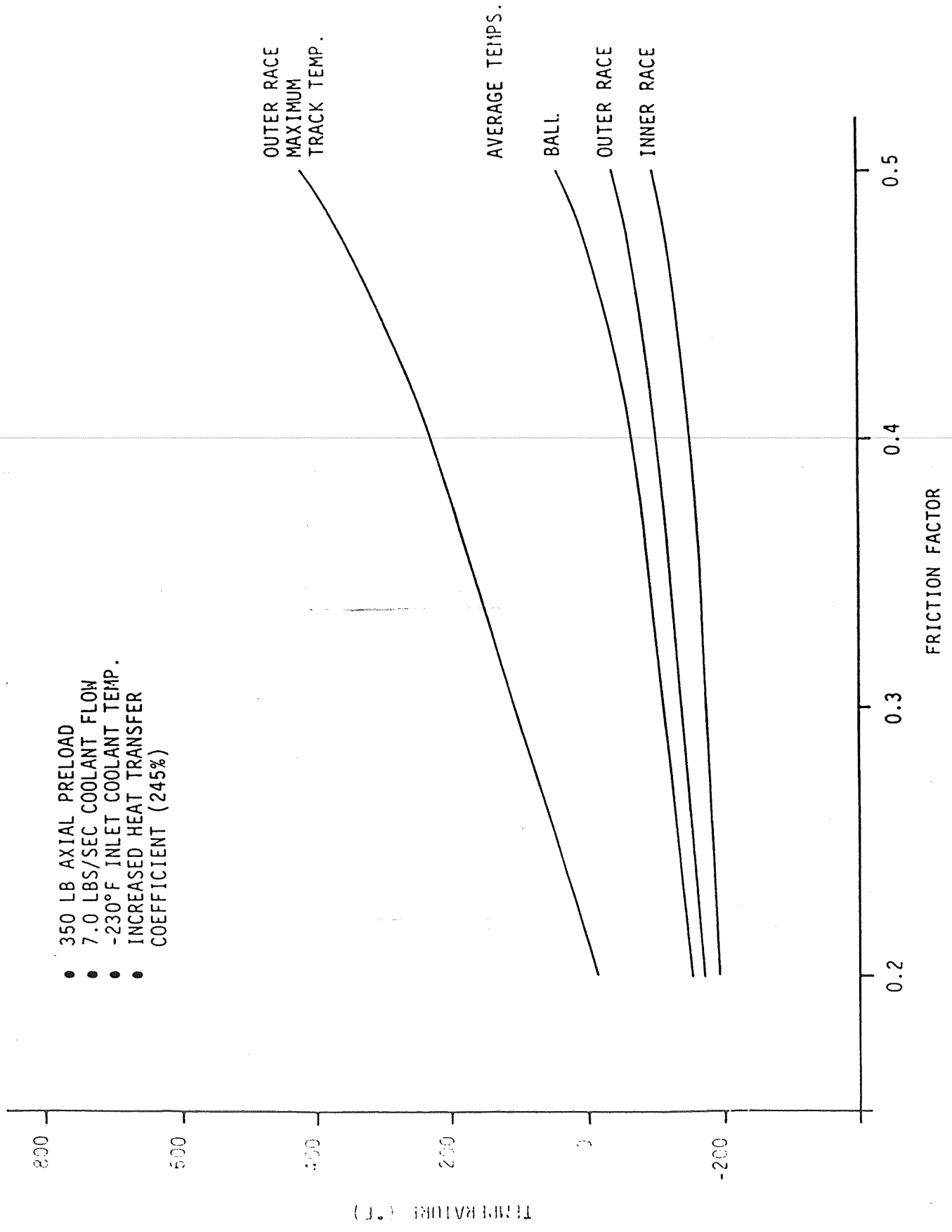
### Effect of Boundary Heat Transfer Coefficient

The more severe cases involving the higher friction factors and preloads were thermally unstable using the nominal heat transfer coefficient. Thus, the heat transfer coefficient was increased to obtain stable solutions over the range of friction factors and preloads considered. Figures 5.2.13 through 5.2.15 show the results of increasing the heat transfer coefficient. The temperatures decrease with increasing heat transfer coefficient. The heat transfer coefficient had a larger effect on the average ball temperature than it did on the average inner and outer race temperatures. This was because the ball has a larger surface to volume ratio exposed to the fluid than do the inner and outer races. Thus, the ball had a larger heat loss increase than did the inner or outer race as the heat transfer coefficient for surface to fluid increased.

The Dittus Boelter equation was used to determine the heat transfer coefficients for the inner and outer races. The Katsnellson equation was used for the ball. The properties were evaluated at the film temperature which is the average of the surface and saturation temperature.

ORIGINAL PAGE IS  
OF POOR QUALITY

FIGURE 5.2.7 45NM BEARING OPERATING TEMPERATURES VS. FRICTION FACTOR



- 350 LB AXIAL PRELOAD
- 7.0 LBS/SEC COOLANT FLOW
- -230°F INLET COOLANT TEMP.
- INCREASED HEAT TRANSFER COEFFICIENT (245%)



FIGURE 5.2.8 45MM BEARING OPERATING TEMPERATURES VS. FRICTION FACTOR

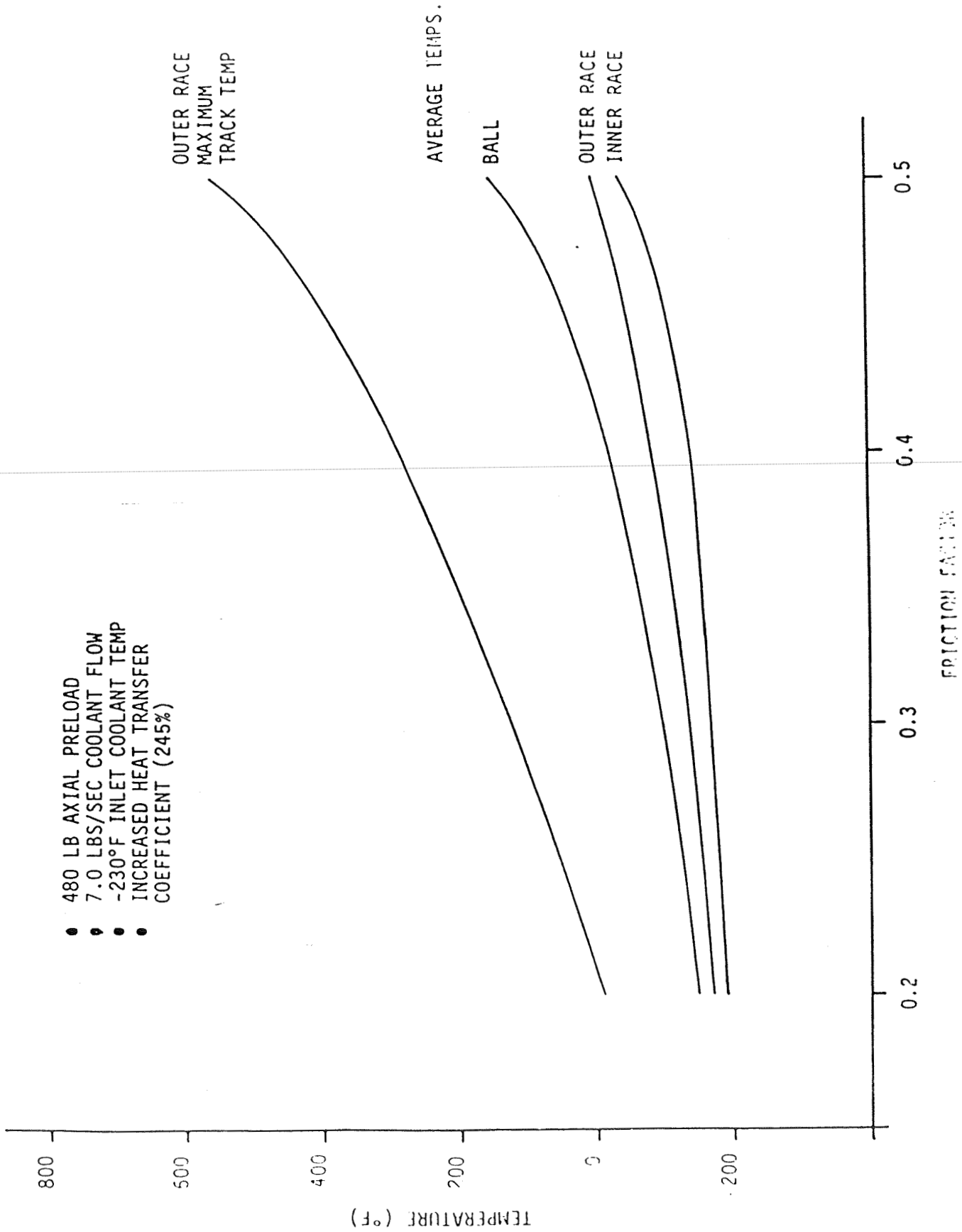


FIGURE 5.2.9 45mm BEARING OPERATING TEMPERATURES VS. FRICTION FACTOR

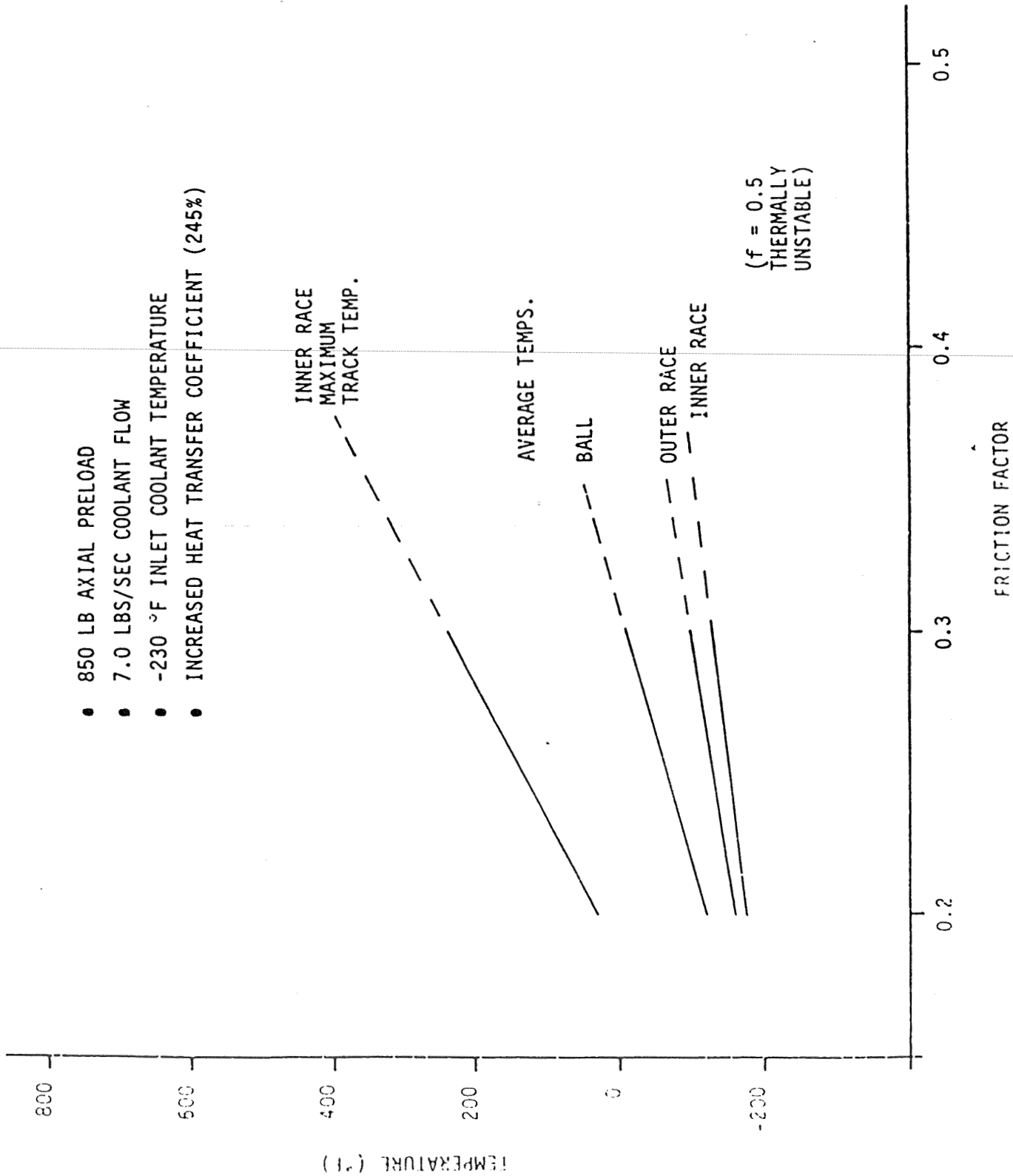


FIGURE 5.2.10 45MM BEARING OPERATING TEMPERATURES VS. FRICTION FACTOR

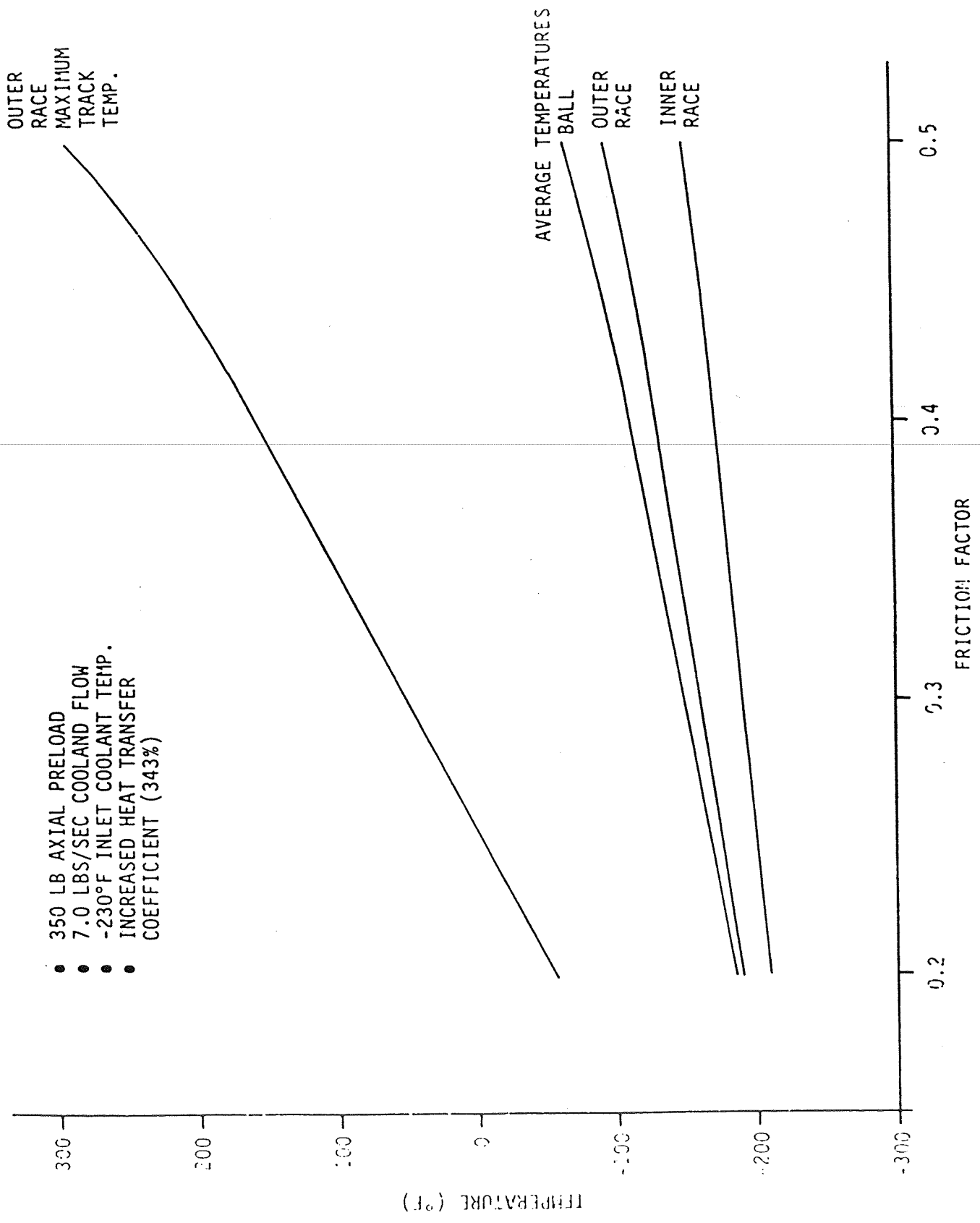


FIGURE 5.2.11 45MM BEARING OPERATING TEMPERATURES VS. FRICTION FACTOR

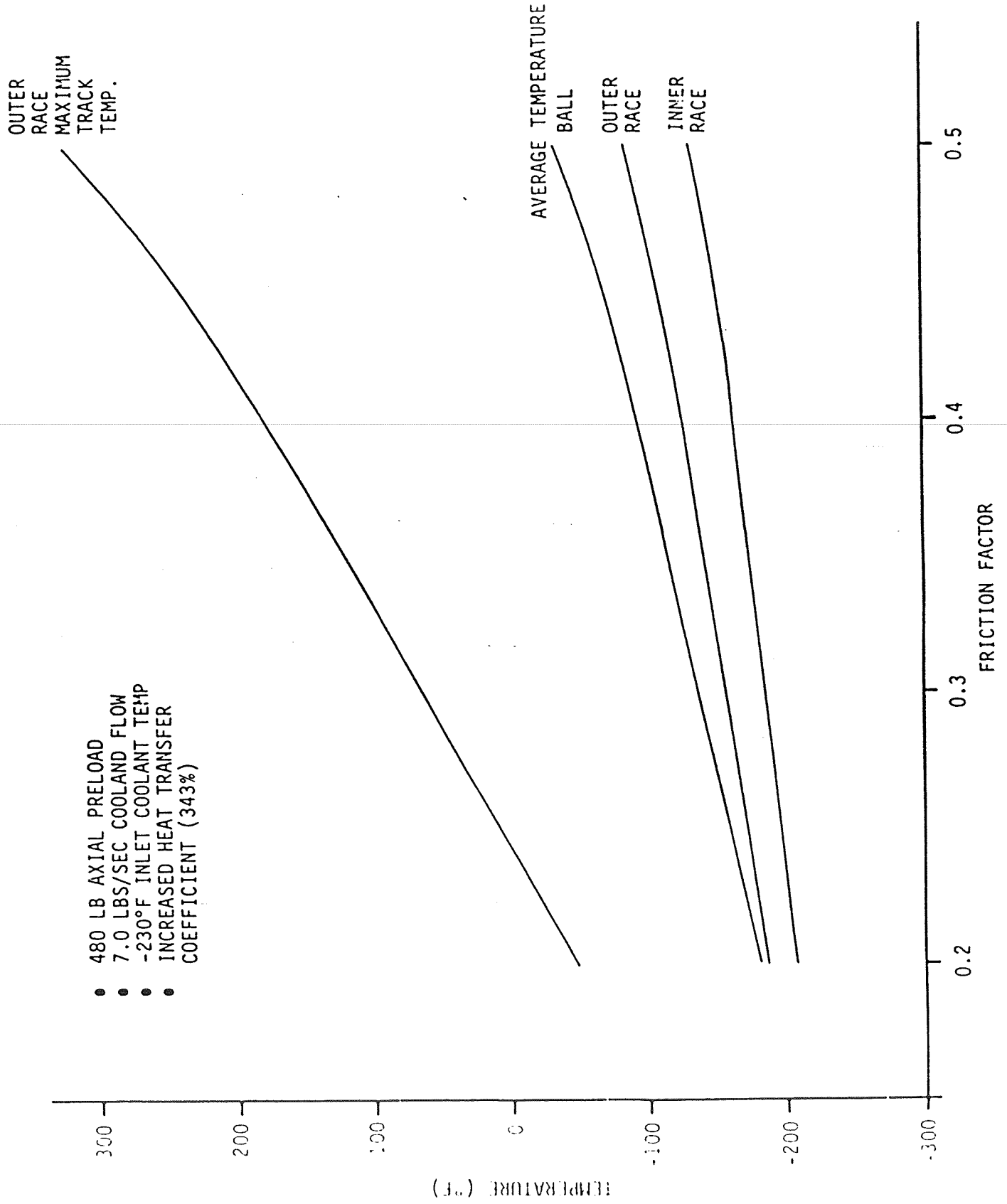


FIGURE 5.2.12 45MM BEARING OPERATING TEMPERATURES VS. FRICTION FACTOR

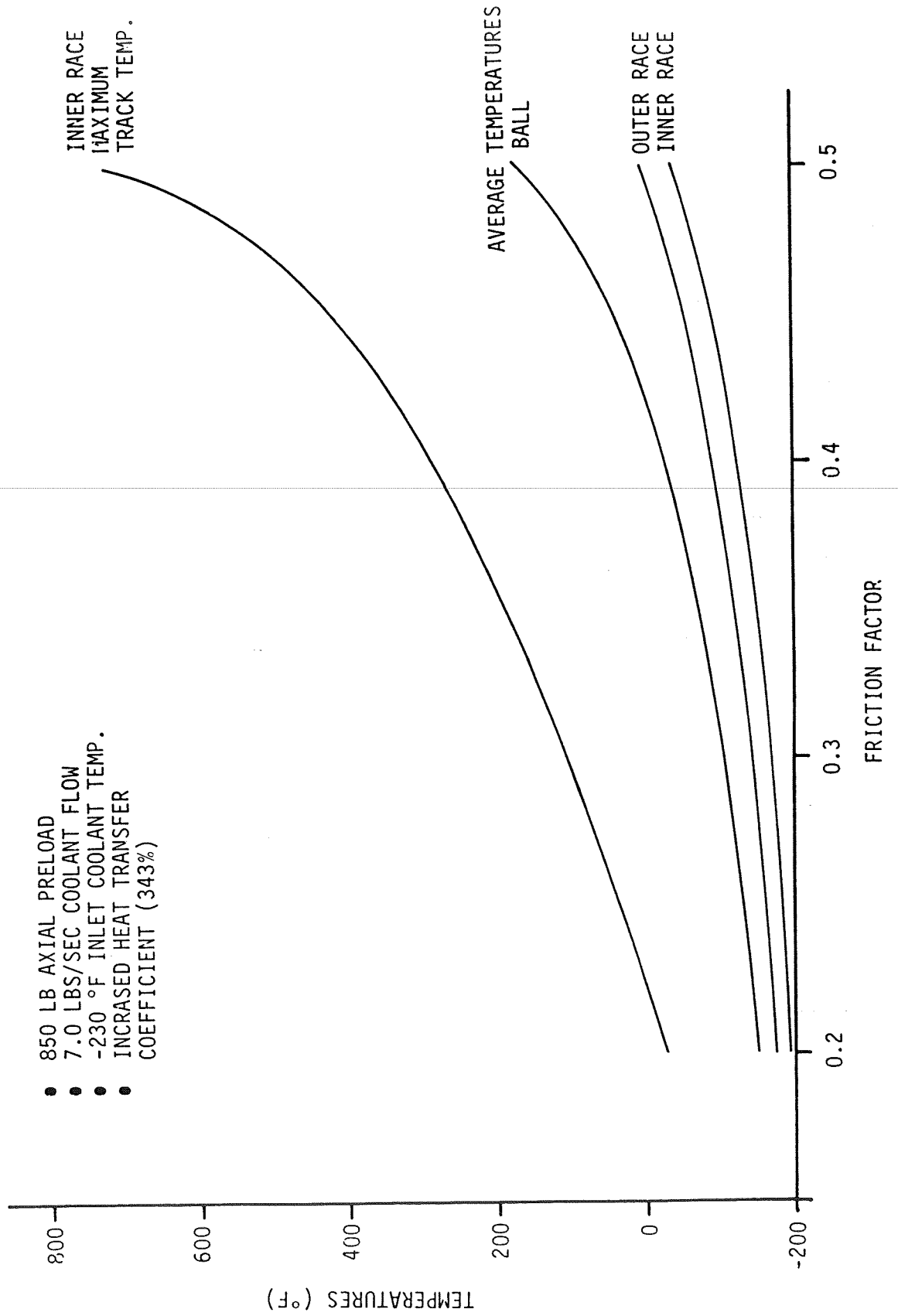


FIGURE 5.2.13 45 MM BEARING OPERATING TEMPERATURES VS. HEAT TRANSFER COEFFICIENT

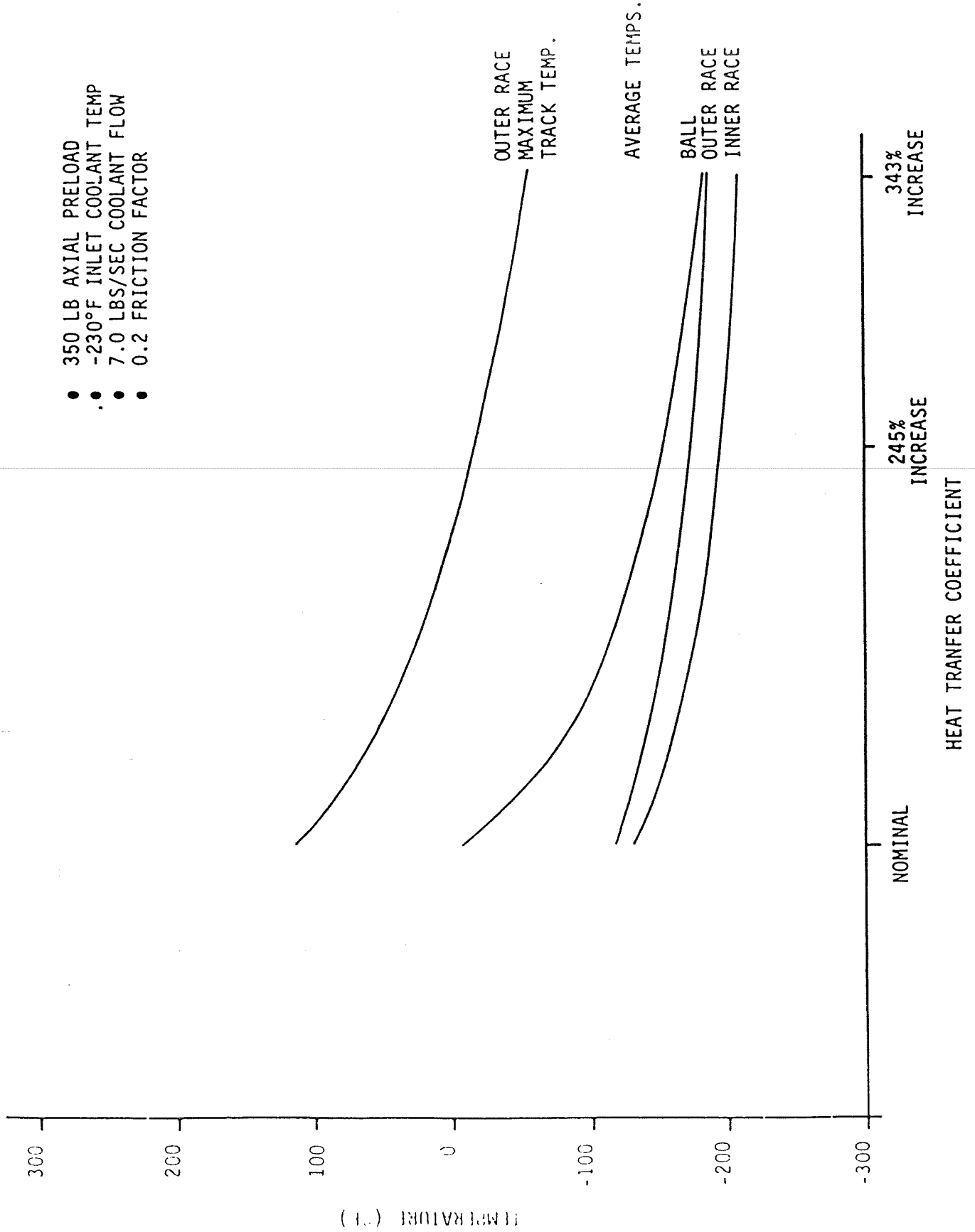


FIGURE 5.2.14  
 45MM BEARING OPERATING TEMPERATURES VS. HEAT TRANSFER COEFFICIENT

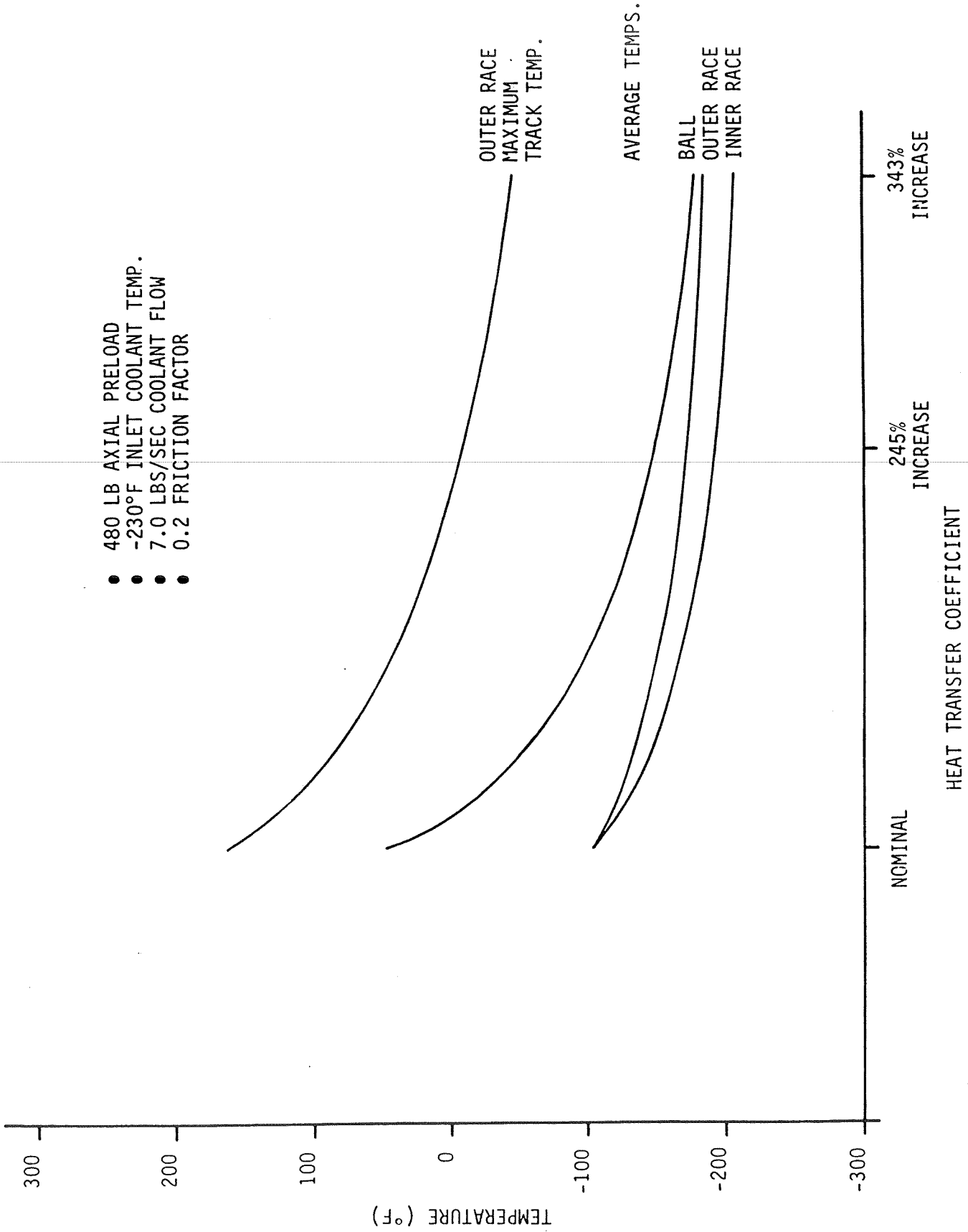
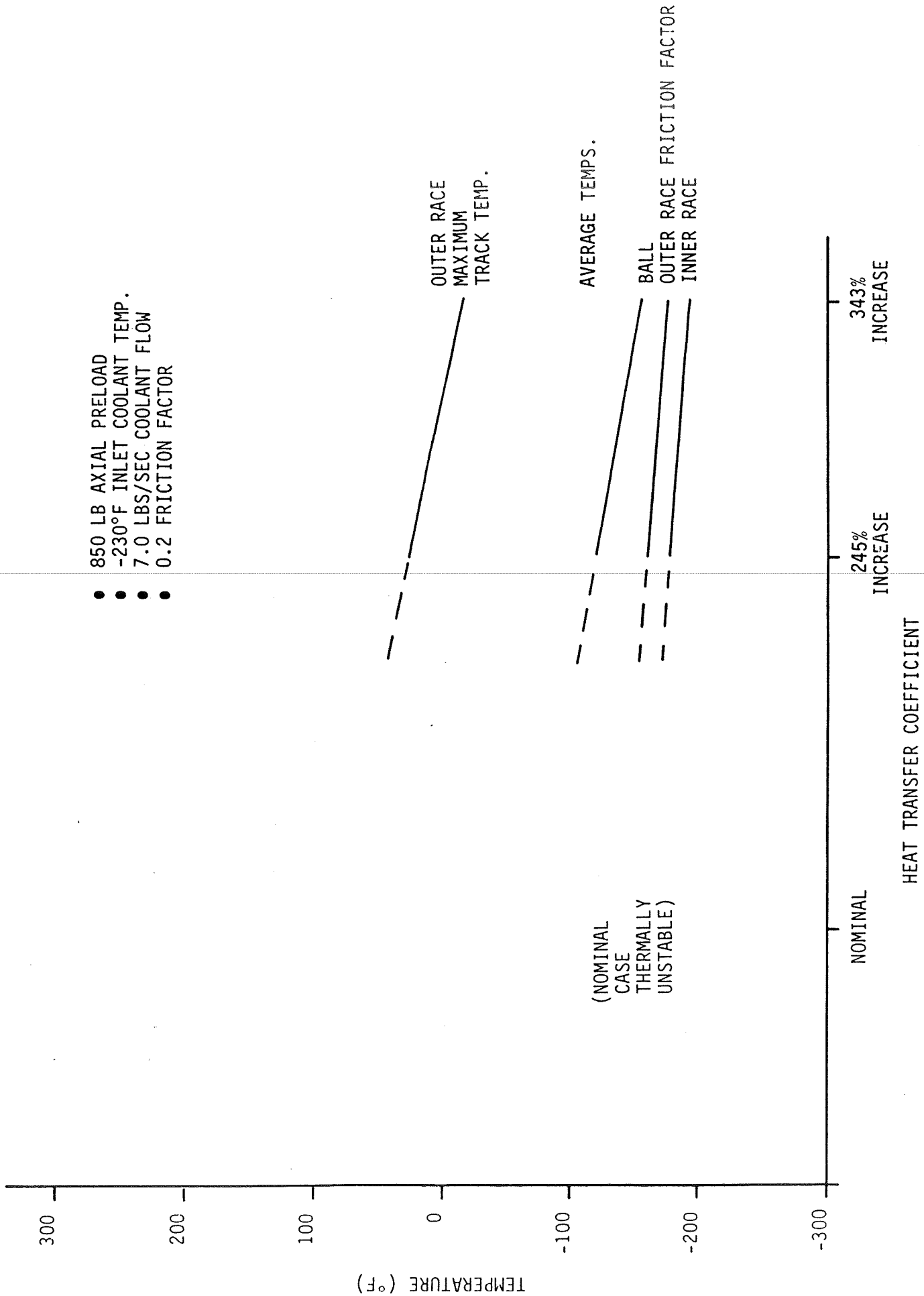


FIGURE 5.2.15  
 45MM BEARING OPERATING TEMPERATURES VS. HEAT TRANSFER COEFFICIENT





## *SRS Technologies*

### Effect of Coolant Flow Rate

Figures 5.2.16 through 5.2.19 show the effect of changing the coolant flow rate. The operating temperatures do not change much over the range of flow rates studied. However, an increase in coolant flow rate could prevent a marginal case from diverging.

### Effect of Inlet Coolant Temperature

The effects of varying inlet temperatures are shown in Figures 5.2.20 through 5.2.23. Two subcooled cases ( $-240^{\circ}\text{F}$  and  $-230^{\circ}\text{F}$ ) and a saturated case ( $T_{\text{sat}} = -214^{\circ}\text{F}$ ) were considered. The coolant was introduced at Bearing 1 and was allowed to increase in temperature while passing through the bearing. For the saturated case, the coolant was introduced at  $-218^{\circ}\text{F}$  and was allowed to increase to the saturation temperature of  $-214^{\circ}\text{F}$  when entering Bearing 2.

The inlet coolant temperature did not have a very significant effect on the bearing operating temperatures. But, lowering the inlet temperature could cause a case that would be thermally unstable to become stable.

### Effect of Outer Race Misalignment

Angular misalignments of the outer race up to 31.5 minutes were studied to determine the effect on bearing operating temperatures. The outer race was tilted so as to place the heaviest loaded ball in the "pinch point". Consequently, the misalignment contributed to the radial loading of the ball. Figure 5.2.24 shows the effect of outer race misalignment for a case using 480 lbs preload, 7.0 lbs/sec flow rate, 0.2 friction factor,  $-230^{\circ}\text{F}$  inlet temperature, and 343% increased heat transfer coefficient. The maximum outer race tilt, that produced a stable solution, was about 29 minutes. This tilt caused the highest stable operating temperatures observed in this analysis. The maximum outer race track temperature was found to be  $1858^{\circ}\text{F}$ . The tilt caused the outer race to heat and expand more than the inner race. Thus, the bearing is able to maintain a sufficient operating clearance for higher ball temperatures.

### Effect of Outer Race to Isolator Clearance

Clearances of 2.6, 1.7, and 1.0 mils between the outer race and isolator were investigated. The heat transfer coefficient was increased 245% of the

FIGURE 5.2.16  
45MM BEARING OPERATING TEMPERATURES VS COOLANT FLOWRATE

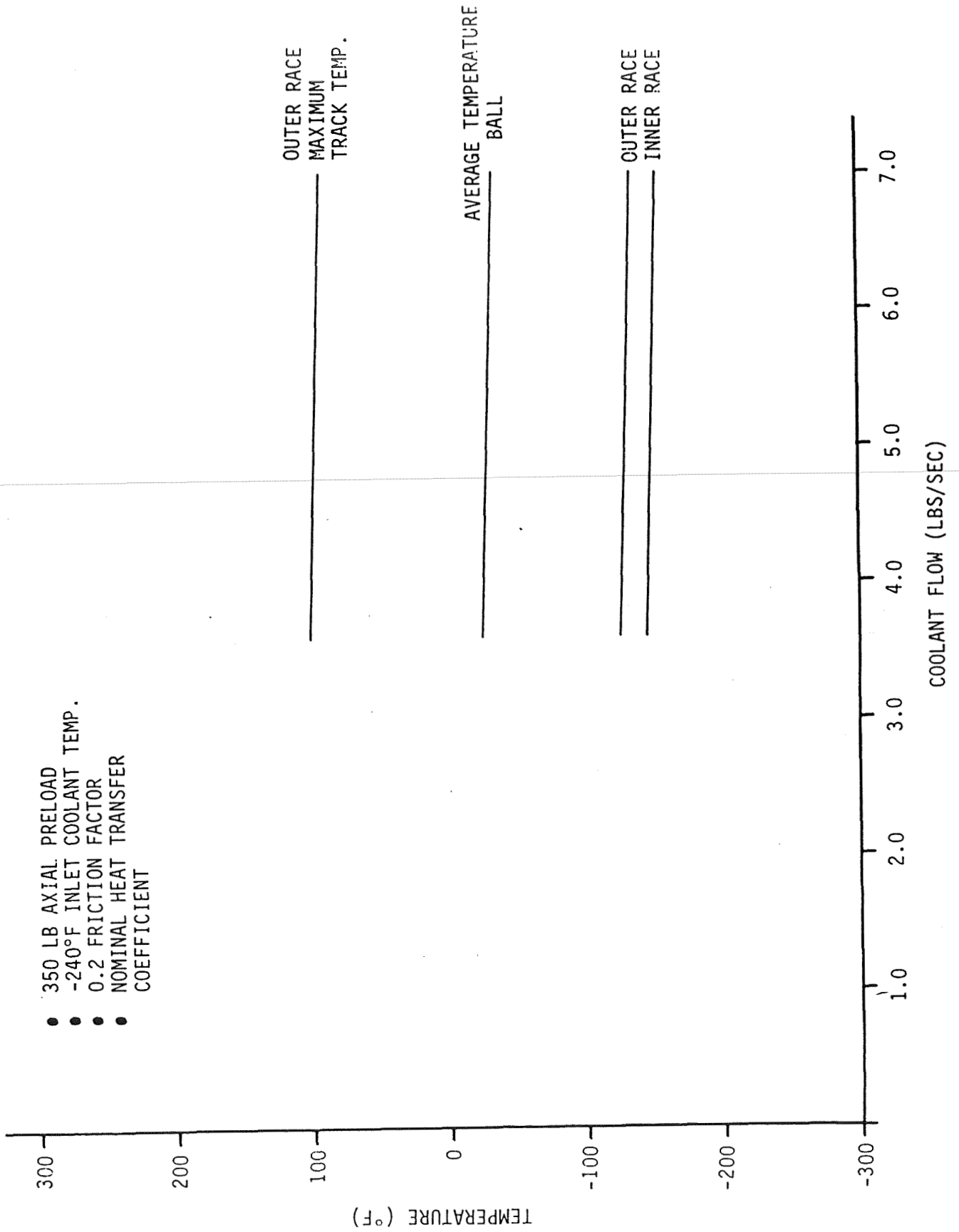


FIGURE 5.2.17 45MM BEARING OPERATING TEMPERATURES VS COOLANT FLOWRATE

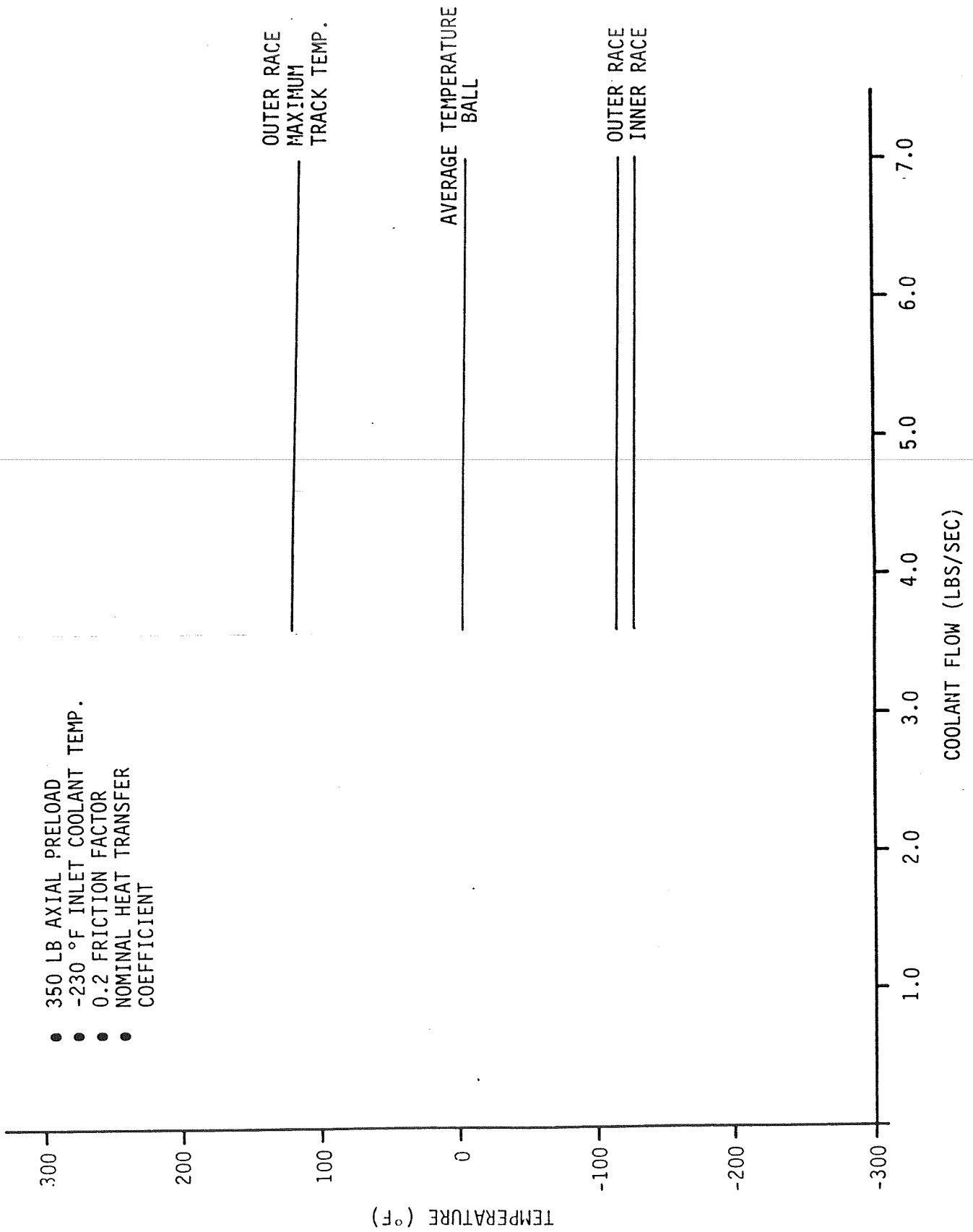


FIGURE 5.2.18 45MM BEARING OPERATING TEMPERATURES VS COOLANT FLOWRATE

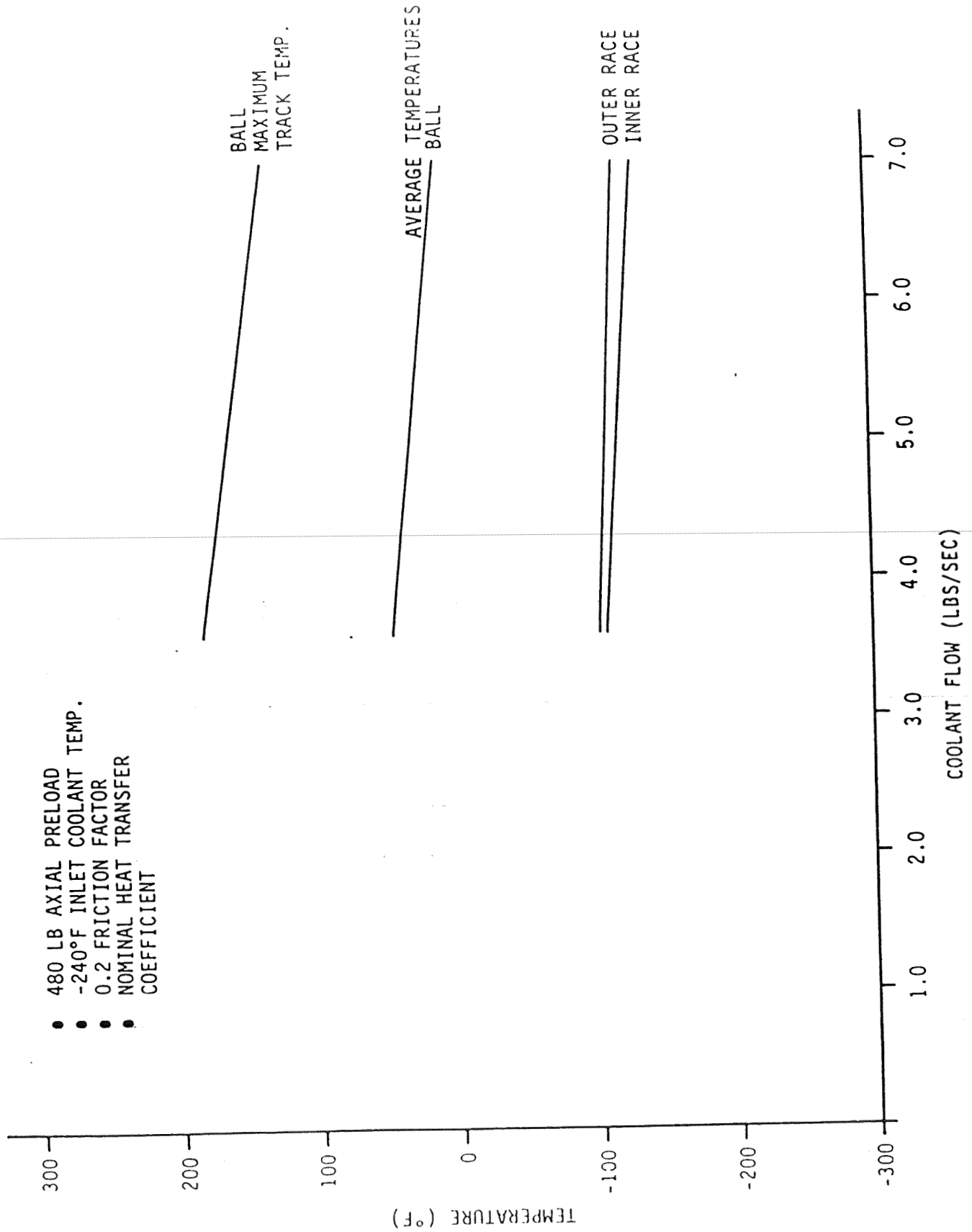


FIGURE 5.2.19 45MM BEARING OPERATING TEMPERATURES VS INLET COOLANT FLOWRATE

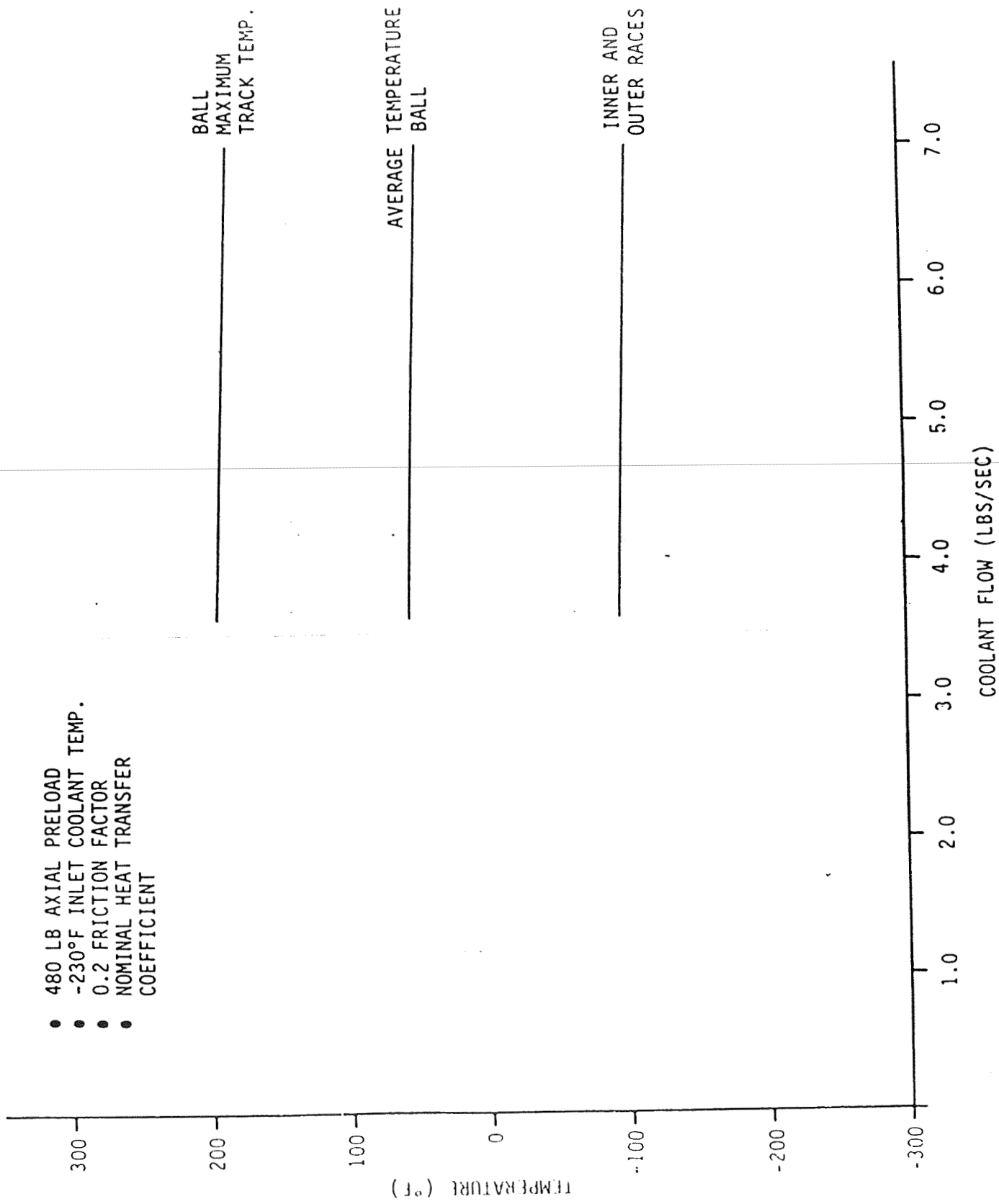


FIGURE 5.2.20 45MM BEARING OPERATING TEMPERATURES VS. INLET COOLANT TEMPERATURE

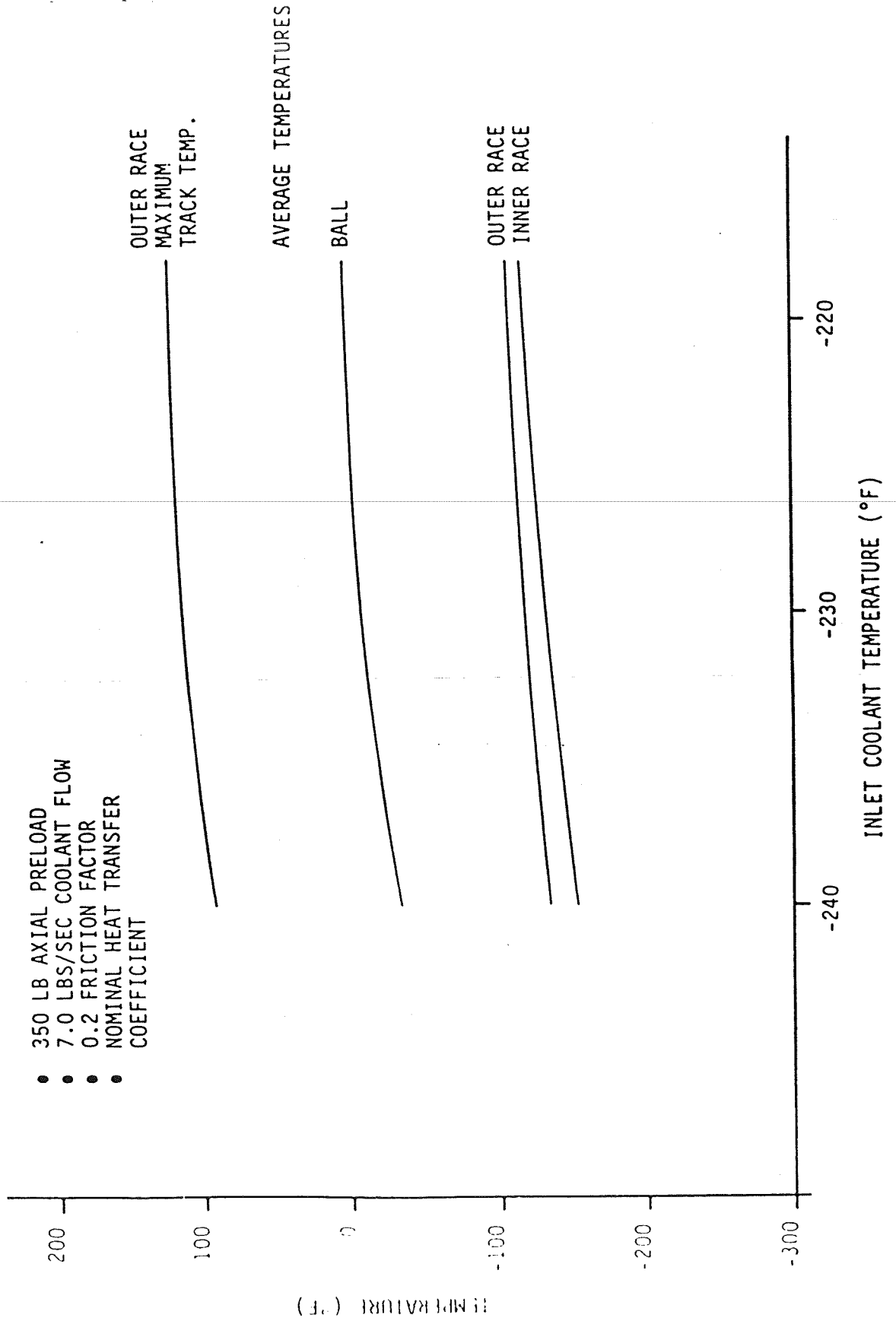


FIGURE 5.2.21 45MM BEARING OPERATING TEMPERATURES VS. INLET COOLANT TEMPERATURE

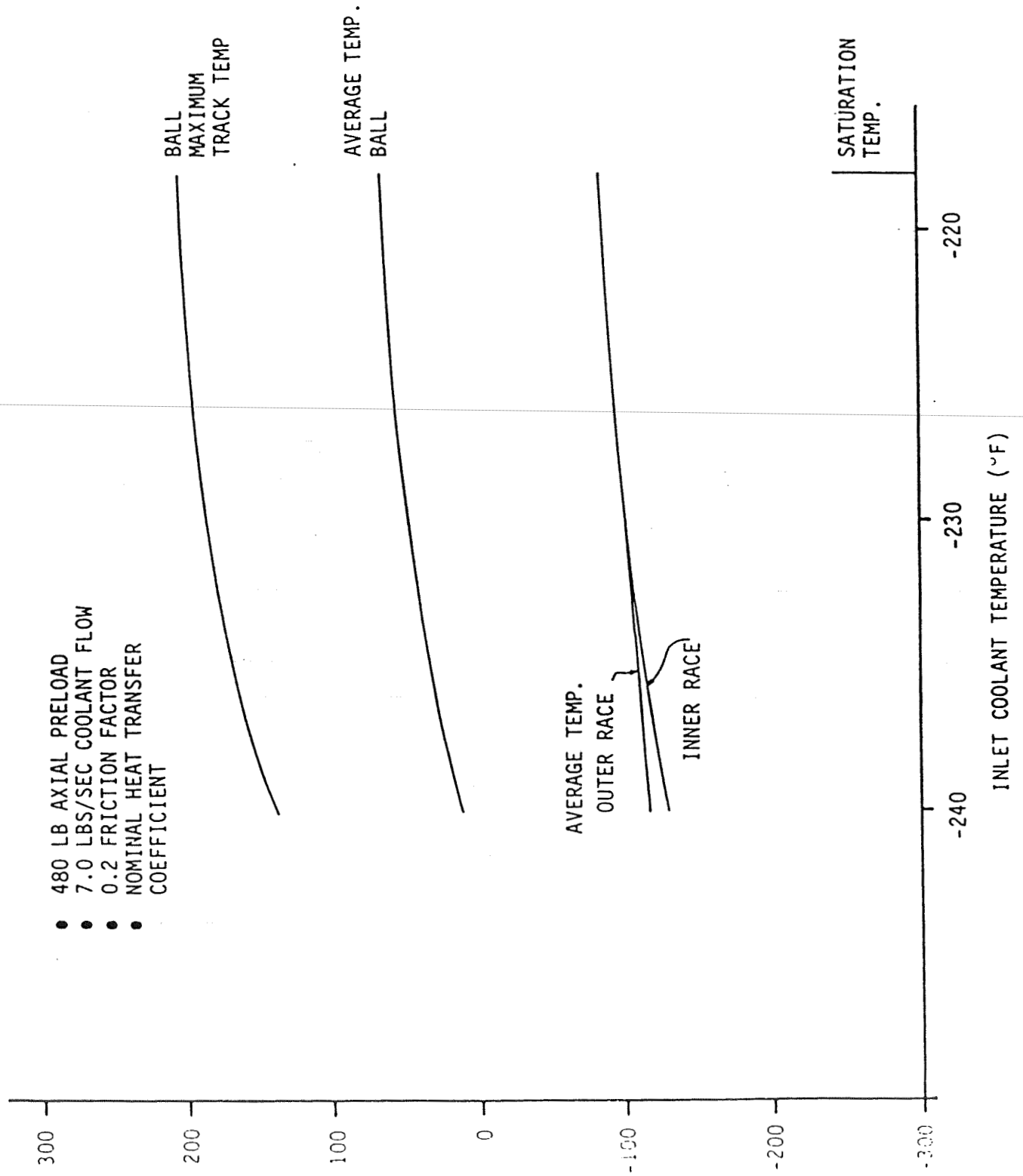


FIGURE 5.2.22 45MM BEARING OPERATING TEMPERATURES VS. INLET COOLANT TEMPERATURE

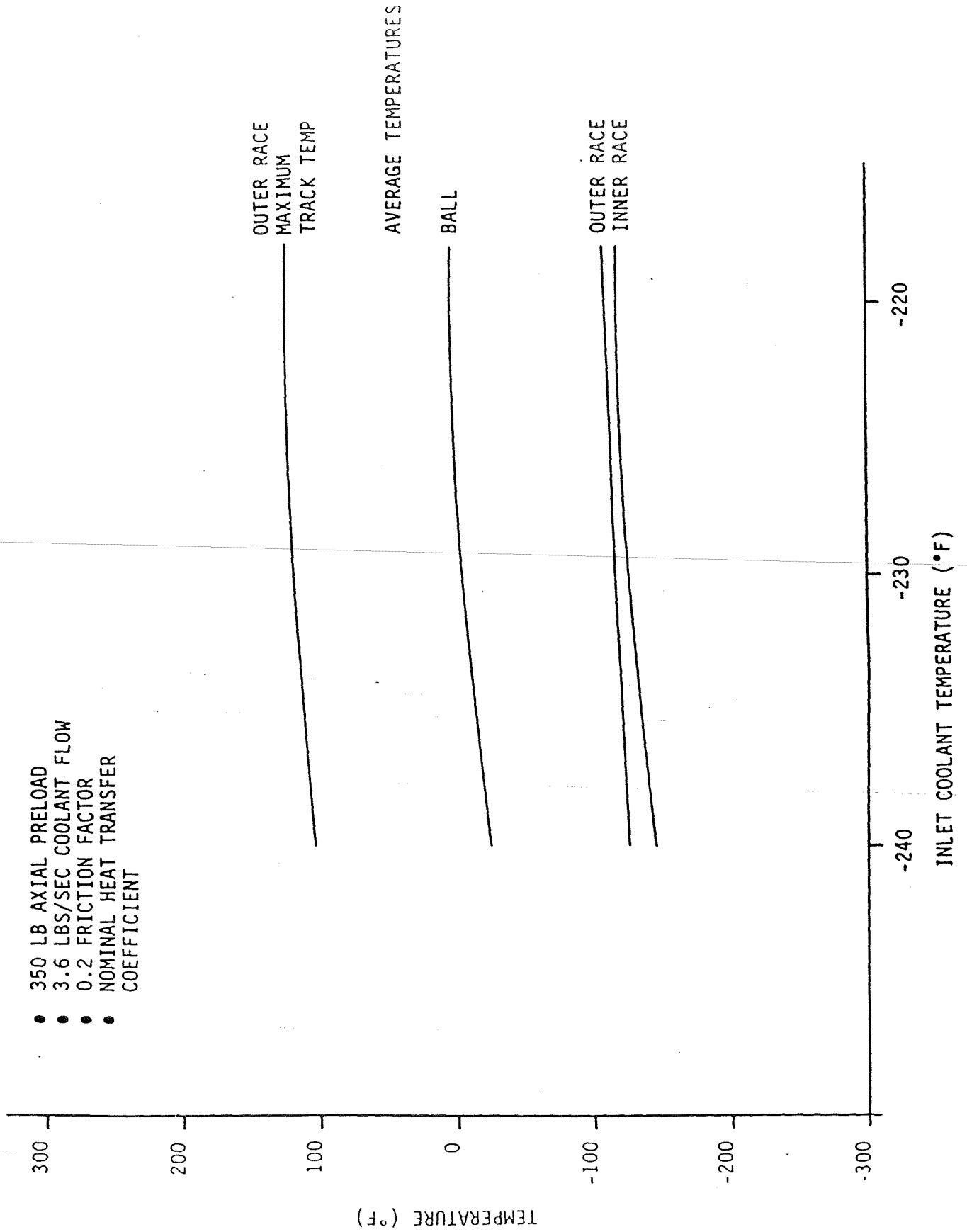




FIGURE 5.2.23 45MM BEARING OPERATING TEMPERATURES VS. INLET COOLANT TEMPERATURE

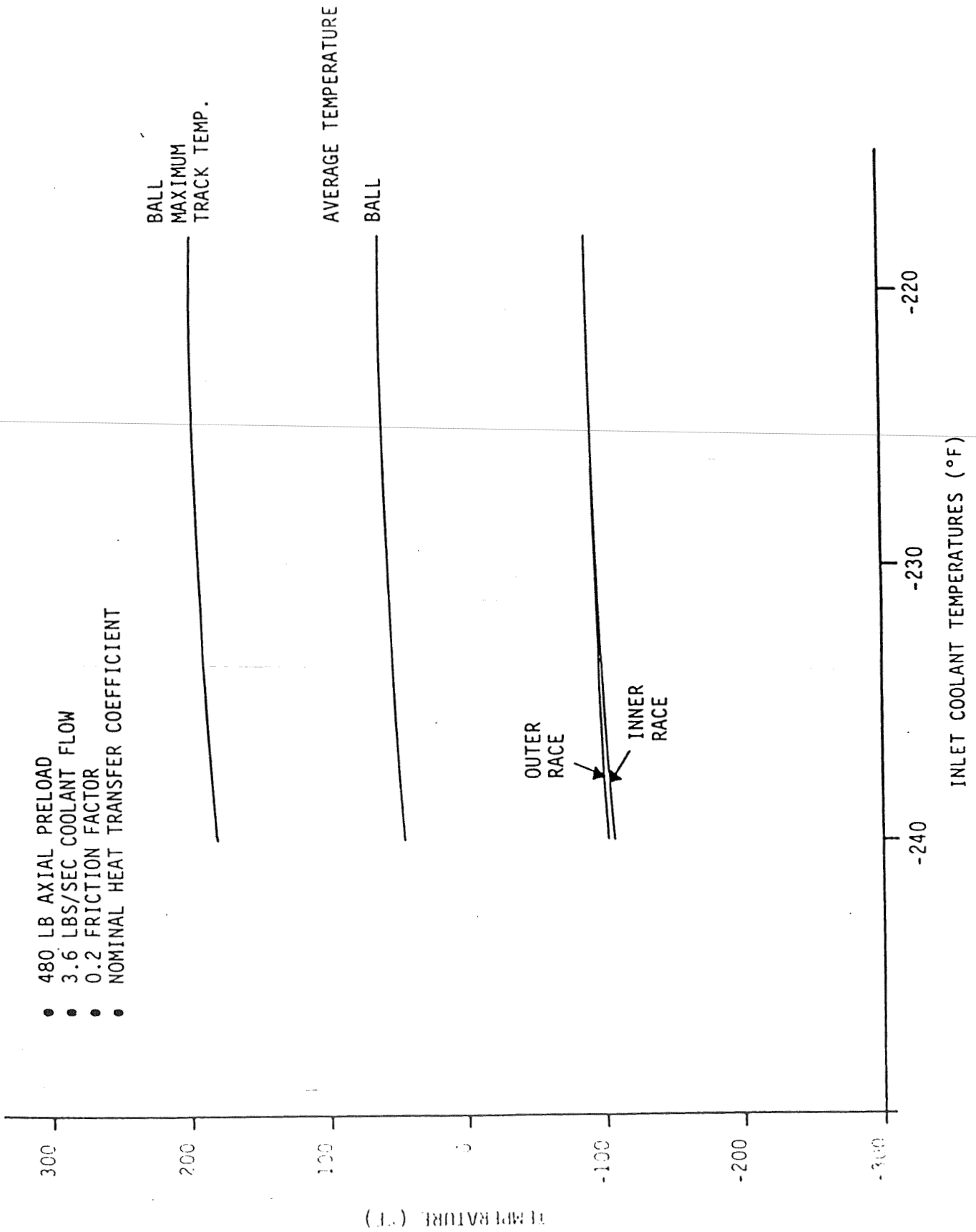
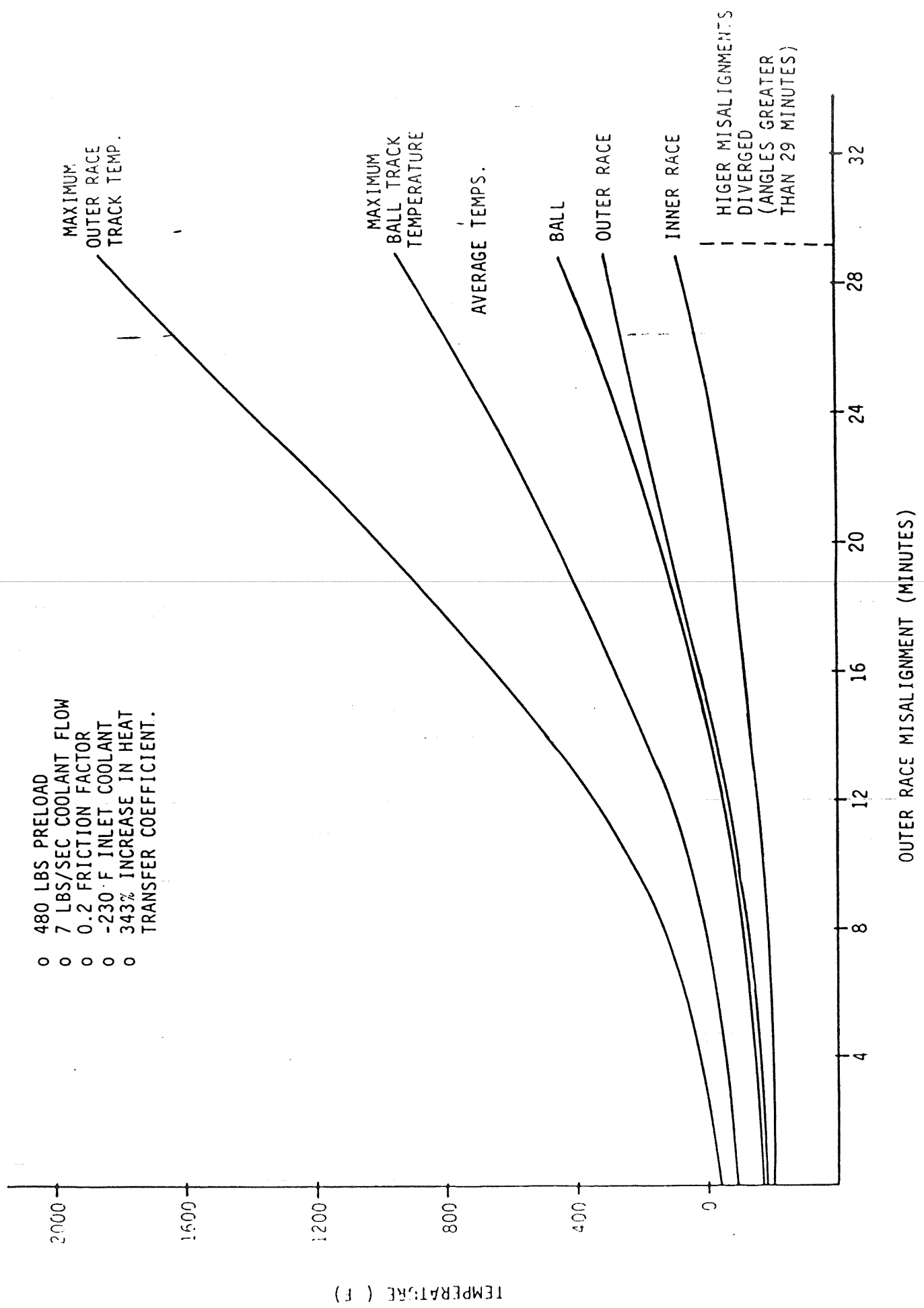


FIGURE 5.2.24 45mm BEARING TEMPERATURES VERSUS OUTER RACE MISALIGNMENT



## *SRS Technologies*

nominal value to obtain stable solutions over the range of parameters studied. The results are shown in Table 5.2.5 and Figure 5.2.25. The clearance, over the range studied, had a small effect on the bearing operating temperatures. The average ball temperature increased 46°F for a decrease in clearance of 2.6 to 1.0 mils at a preload of 850 lbs. However, these are radial loaded conditions and the effects could be more severe under axial load. The bearing outer race could be restricted from moving in the axial direction since the operating clearance between the outer race and isolator is zero for these conditions.

### Effect of Thermal Isolation of the Outer Race

The effect of thermally isolating the outer race from the isolator was determined. The results are shown in Table 5.2.6. The temperature increase was very slight. The small increase indicates that most of the heat generated is transferred to the coolant and very little is transferred through the bearing isolator.

### Coolant Quality

The coolant quality profile was determined for the saturated cases using flow rates of 7.0 and 3.6 lbs/sec. The profiles are shown in Figures 5.2.26 and 5.2.27. The quality was calculated as the mass of vapor per total mass of coolant. The mass of vapor was determined from the amount of heat transferred to each fluid node. The fluid quality was decreased by approximately 70% by increasing the flow rate from 3.6 to 7.0 lbs/sec. Figure 5.2.26 shows that no vapor was generated in Bearing 1 for the higher flow rate.

TABLE 5.2.5 EFFECT OF OUTER RACE TO ISOLATOR CLEARANCES (45mm BEARING)

OUTER RACE CLEARANCE	BEARING AXIAL PRELOAD (LBS)																	
	350				480				850									
	AVERAGE TEMPERATURE (°F)		MAXIMUM TRACK TEMPERATURE (°F)		AVERAGE TEMPERATURE (°F)		MAXIMUM TRACK TEMPERATURE (°F)		AVERAGE TEMPERATURE (°F)		MAXIMUM TRACK TEMPERATURE (°F)							
INNER RACE	BALL	OUTER RACE	INNER RACE	BALL	OUTER RACE	INNER RACE	BALL	OUTER RACE	INNER RACE	BALL	OUTER RACE	INNER RACE	BALL	OUTER RACE				
2.6 mils	-197	-158	-173	-64	-67	-17	-193	-150	-171	-44	-50	-9	-179	-120	-160	24	8	27
1.7 mils	-195	-154	-172	-54	-58	-11	-190	-144	-168	-29	-37	1	-171	-106	-153	62	40	53
1.0 mils	-192	-148	-169	-39	-45	-2	-184	-130	-164	-1	-13	15	-154	-74	-142	123	94	90

Flowrate = 7.0 lbs/sec  
 Friction Factor = 0.2  
 245% Increase in Heat Transfer Coefficient  
 Inlet Coolant Temperature = -230°F

FIGURE 5.2.25

OUTER RACE TO ISOLATOR CLEARANCE  
VS. COMPONENT TEMPERATURES

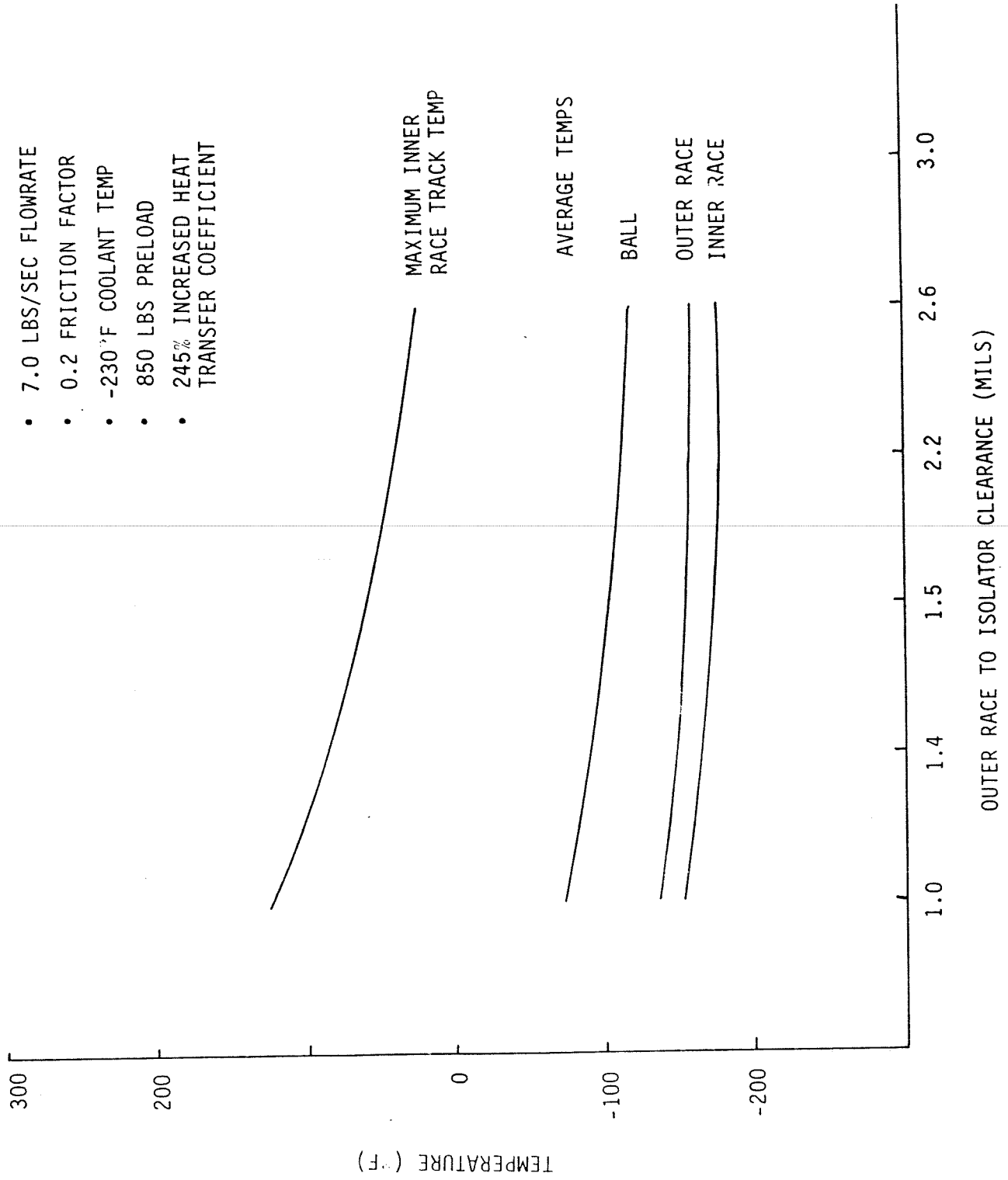
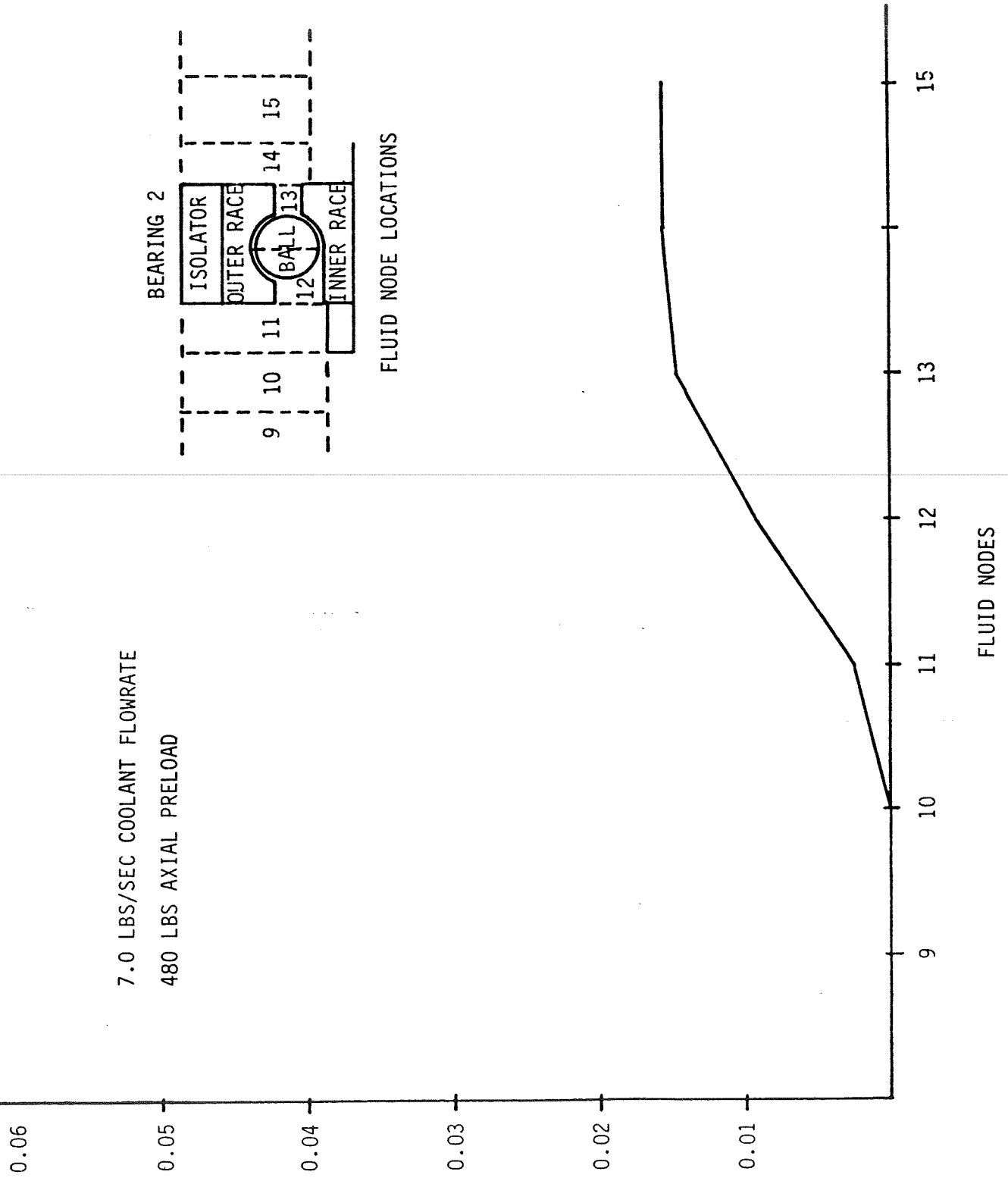


TABLE 5.2.6 EFFECTS OF THERMAL ISOLATION OF BEARING ISOLATOR (45mm BEARING)

HEAT TRANSFER BETWEEN ISOLATOR & OUTER RACE		BEARING AXIAL PRELOAD (LBS)																	
		350				480				850									
		AVERAGE TEMPERATURE (°F)			MAXIMUM TRACK TEMPERATURE (°F)			AVERAGE TEMPERATURE (°F)			MAXIMUM TRACK TEMPERATURE (°F)								
		INNER RACE	BALL RACE	OUTER RACE	INNER RACE	BALL RACE	OUTER RACE	INNER RACE	BALL RACE	OUTER RACE	INNER RACE	BALL RACE	OUTER RACE						
With		-197	-158	-173	-64	-67	-17	-193	-150	-171	-44	-50	-9	-179	-120	-160	24	8	27
Without		-198	-158	-165	-66	-68	-11	-193	-150	-162	-45	-50	-2	-180	-122	-151	15	1	32

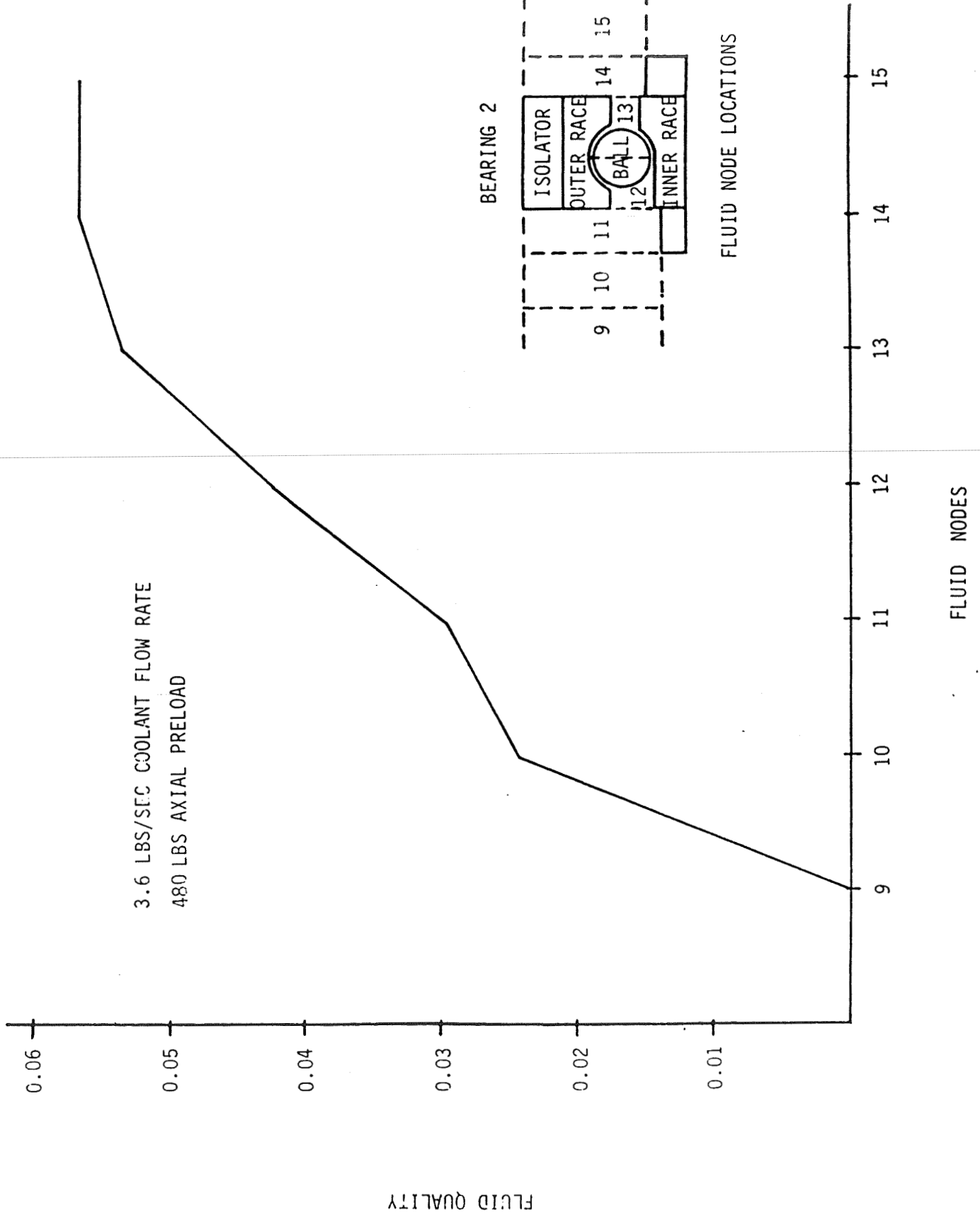
Flowrate = 7.0 lbs/sec  
 Friction Factor = 0.2  
 245% Increase in Heat Transfer Coefficient  
 Inlet Coolant Temperature = 230°F

FIGURE 5.2.26 FLUID QUALITY THROUGH BEARING #2



FLUID QUALITY

FIGURE 5.2.27 FLUID QUALITY THROUGH BEARING #2





# *SRS Technologies*

## 6.0 CONCLUSIONS AND RECOMMENDATIONS

The turbopump bearing component temperatures are very sensitive to load, contact friction, and fluid/boundary heat transfer coefficients. Alignment of the outer race was found to be critical as bearing temperatures are very sensitive to this parameter. For the majority of the conditions evaluated, the operating clearance between the outer race and isolator was lost. Although, for the radially loaded conditions, the effect of isolator clearance on bearing temperatures was nominal, the loss of clearance would be considerably more detrimental for axial load transients. While not as sensitive to coolant flow (according to analysis) and coolant quality, these parameters can become important for marginal operating conditions. According to the analysis, the internal operating clearance of the 45 mm bearing must be at least ~3.9 mils to maintain a thermally stable operating condition.

Since the bearing temperatures are very sensitive to heat transfer coefficients, further work should be done to investigate the possible effects of the internal flow field characteristics or fluid/boundary heat transfer. In addition, recent tests of the Bearing and Seal Materials Tester showed a higher dependence of bearing temperature on coolant flow than was predicted by analysis. This inconsistency in the analysis should be investigated. Improved methods for cooling the bearings, i.e., under race cooling, introducing the coolant between the bearings, etc., should be modeled and evaluated for improved efficiency in cooling the LOX turbopump bearings.



555 SPARKMAN DRIVE/SUITE 1406  
HUNTSVILLE, ALABAMA 35816-3425

(205) 830-0375

SYSTEMS TECHNOLOGY DIVISION

January 6, 1986  
OL86-1249

TO: DISTRIBUTION

SUBJECT: Final Report for Space Shuttle Main Engine (SSME) LOX Turbopump  
Pump-End Bearing Analysis

PREPARED FOR: Mr. Fred Dolan  
Materials and Processes Laboratory  
Engineering Physics Division  
George C. Marshall Space Flight Center  
Marshall Space Flight Center, AL 35812

SUBMITTED BY: SRS Technologies  
Systems Technology Division  
555 Sparkman Drive; Suite 1406  
Huntsville, AL 35805

CONTRACT NO.: NAS8-36183 Modification No. 6.

DATE OF PUBLICATION: January 6, 1986

The enclosed R&D Final Report provides a description of the work performed under the subject contract modifications.

Sincerely,

SRS TECHNOLOGIES  
Systems Technology Division

A handwritten signature in cursive script that reads "Joe C. Cody".

Joseph C. Cody  
Project Engineer

JCC/kct

Enclosures: as stated

DISTRIBUTION: George C. Marshall Space Flight Center  
Mr. Fred J. Dolan, EH14 (6 Copies + Repro.)  
Mr. Schwingamer, EH01  
Mr. Riggs, EP23  
Mr. McCarty, EP21  
Mr. Geotz, EE51  
Mr. Lombardo, SA53  
Mr. G. Smith, SA51  
Mr. Lovingood, SA51  
AT01  
AS24D (3 Copies)  
EH11  
AP29-F  
EM13B-21  
BF30  
CC01/Wofford

NASA Scientific and Technical Information Center  
ATTN: Accessioning Department (1 Copy + Repro.)

DCASMA

# *SRS Technologies*

## FOREWORD

This report was prepared by SRS Technologies under Contract NAS8-36183 Modification Number 6 for the George C. Marshall Space Flight Center of the National Aeronautics and Space Administration. The work was administered under the technical direction of the Engineering Physics Division of the Materials and Processes Laboratory with Mr. Fred F. Dolan as Project Manager. This report describes the work accomplished in accordance with Contract Modification Number 6. Mr. Joseph C. Cody was the SRS Project Engineer. A list of the key contributors is shown below.

Mr. David Marty  
Dr. Alok Majumdar  
Mr. Bruce K. Tiller

